TRANSIENT TEMPERATURE MODELING FOR WELLBORE FLUID UNDER STATIC AND DYNAMIC CONDITIONS

A Thesis

by

MUHAMMAD ALI

Submitted to the Office of Graduate and Professional Studies of
Texas A&M University
in partial fulfillment of the requirements for the degree of

MASTER OF SCIENCE

Chair of Committee,	Abu Rashid Hasan
Committee Members,	Hadi Nasrabadi
	Yuefeng Sun
Head of Department,	A. D. Hill

May 2014

Major Subject: Petroleum Engineering

ABSTRACT

Modeling flowing wellbore fluid transient temperature is important in many petroleum engineering problems, including, pressure transient testing, flow assurance and wellbore integrity during production, preservation of drilling equipment integrity for geothermal wells and prediction of injection fluid temperatures.

In this thesis, development and usage of three models for transient fluid temperature are presented. Two models predict transient temperature of flowing fluid under separate flow configurations and one is for a static fluid column. Additionally, an improvement to an existing transient temperature solution is given.

The *transient rate model* predicts the transient temperature when a flow rate, during production, is changed from some initial value to a new one. This model is particularly useful for pressure transient tests involving multiple disparate constant flow rates where bottomhole pressure has to be calculated from the wellhead pressure. Dependence of fluid density on variable temperature during the test necessitates that effects of unsteady temperature changes are taken into account for accurate calculation of downhole pressure.

The *single rate injection model* predicts transient temperature of wellbore fluids during injection operations. This model can help in design of acidizing treatments by allowing

users to calculate the time required to cool down the well with water pre-flush. This model can also be used for calculation of depth of effectiveness of wax removal treatment, in case of hot oil injection.

Very high temperatures during drilling operations can deteriorate mud rheological properties. The c*onduction model* lets the user calculate the time window available for taking corrective actions after an accidental cessation of mud circulation occurs.

Method of Laplace transform enabled solution of a temperature distribution equation to create the transient rate model and the injection model. Conduction model was developed by solving the transient heat conduction equation for a multilayer cylinder with mud in annulus and tubing analogous to two layers of the cylinder. All solutions were implemented using conventional spreadsheet software with rudimentary programming.

DEDICATION

To my parents, wife and siblings.

ACKNOWLEDGEMENTS

I would like to thank Dr. A.R. Hasan whose guidance enabled me to complete this thesis. His deep insights helped me solve all the problems related to research. He also mentored me through all the ups and downs of my life during graduate studies. I could not even imagine having a better research adviser. I also acknowledge his valuable financial support during the course of my studies.

I also want to thank Petroleum Engineering Department for providing me financial assistance in the form of Teaching Assistantships.

Thanks also go to Mr. Shah Kabir at Hess Corporation for his valuable input during the research.

I want to thank my father who always encouraged me to pursue my dreams. I could not thank my mother enough for her unparalleled emotional support. I also want to thank my wife for her love and patience.

I also want to thank my research group members, friends and fellow Aggies who made my research a memorable experience.

NOMENCLATURE

a_{in}	Coefficients of Bessel functions
A	Lumped parameter defined by Eq. A-82, hr^{-1}
A'	Lumped parameter defined by Eq. A-81, hr^{-1}
b_{in}	Coefficients of Bessel functions
$\check{B}$	Parameter defined by Eq. A-60, dimensionless
$\hat{B}$	Parameter defined by Eq. A-27, dimensionless
C_J	Joule-Thomson coefficient, °F/(lb_f/ft^2)
c_p	Tubing fluid heat capacity, Btu/lbm °F
C_T	Thermal storage parameter, dimensionless
g	Gravitational acceleration, ft/sec^2
g_c	Conversion factor, 32.17 (lbm-ft)/lbf/sec^2
g_G	Geothermal gradient, °F/ft
H	Heaviside function
k_{actual}	Actual thermal conductivity of mud, Btu/hr.ft.°F
k_{eff}	Effective thermal conductivity of mud, Btu/hr.ft.°F
k_e	Formation thermal conductivity, Btu/hr.ft.°F
J	Conversion factor, 778 ft.lbf/Btu
J_0	Bessel function of the first kind of order zero
L	Length of flow string, ft

L_R	Relaxation length parameter given by Eq. A-30, ft^{-1}
L'_R	Relaxation length parameter given by Eq. A-30 after rate change
m	Mass of fluid per unit length, lbm/ft
m'	Mass of fluid per unit length after a flow rate change, lbm/ft
$\breve{m}$	Parameter defined by Eq. 20, dimensionless
$\hat{m}$	Parameter defined by Eq. 8, dimensionless
r	radial coordinate
r_{to}	Outside tubing radius, ft
r_w	Wellbore radius, ft
t	Producing/injection time, hr
$t_{cooling}$	Time required for cooling entire wellbore depth, hr
t_D	Dimensionless time
T_D	Dimensionless temperature
T_{ei}	Undisturbed formation temperature at any depth, °F
T_{eibh}	Undisturbed formation temperature at bottomhole, °F
T_f	Tubing fluid temperature, °F
T_{fwh}	Tubing fluid temperature at wellhead, °F
T_{ss}	Steady state temperature of tubing or annulus mud, °F
T_{sur}	Undisturbed formation temperature at wellhead, °F
U_{to}	Overall heat transfer coefficient, $Btu/hr.ft^2.°F$
v	Velocity of fluid, ft/hr
w	Mass rate of tubing fluid, lbm/hr

w'	Mass rate of tubing fluid after a flow rate change, lbm/hr
Y_0	Bessel function of the second kind of order zero
z	Well depth, ft
$z_{effective}$	Depth of effectiveness of hot injection treatment, ft
z'_{inj}	Parameter defined by Eq. A-56, ft
z'_{prod}	Parameter defined by Eq. 9, ft
α_e	Thermal diffusivity of formation, ft^2/hr
α	Thermal diffusivity, ft^2/sec
ε	Multiplier for mud thermal conductivity, dimensionless
λ	Eigenvalue
ϕ	Lumped parameter defined by Eq. A-33, °F/ft
ϕ'	Lumped parameter defined by Eq. A-33 after a flow rate change
ψ	Lumped parameter defined by Eq. A-12, °F/ft
ψ'	Lumped parameter defined by Eq. A-83, °F/ft

TABLE OF CONTENTS

Page

ABSTRACT ii

DEDICATION iv

ACKNOWLEDGEMENTS v

NOMENCLATURE vi

TABLE OF CONTENTS ix

LIST OF FIGURES xi

LIST OF TABLES xii

Chapter I INTRODUCTION 1

- Single and Transient Rate Production 1
- Single Rate Injection 3
- Mud Temperature after Cessation of Circulation 4
- Proposed Solutions 5

Chapter II LITERATURE REVIEW 6

- Single and Transient Rate Production 6
- Single Rate Injection 8
- Mud Temperature after Cessation of Circulation 8

Chapter III SINGLE RATE PRODUCTION 10

- Introduction 10
- Example Case and Discussion 12
- Summary 19

Chapter IV TRANSIENT RATE PRODUCTION 20

- Introduction 20
- Example Case and Discussion 22
- Summary 26

Chapter V SINGLE RATE INJECTION 27

Introduction 27
Example Case and Discussion 29
Summary 38

Chapter VI TRANSIENT TEMPERATURE OF STATIC MUD AFTER CESSATION OF CIRCULATION 40

Introduction 40
Example Case and Discussion 42
Summary 49

Chapter VII SUMMARY 51

REFERENCES 54

APPENDIX 59

Single Rate Production 59
Single Rate Injection 65
Transient Rate Production 71
Transient Temperature of Mud after Cessation of Circulation 76
Non-homogeneous Steady State Problem 78
Transient Problem 79
Orthogonality Condition Proof 81

LIST OF FIGURES

Page

Figure 1. Comparison of temperature profiles of Bahonar et. al (2011) and this study...13

Figure 2. Comparison of temperature profiles of Hasan et. al (2005) and this study 16

Figure 3. Comparison of Logistic function and Heaviside function at t=0.2778 hr 17

Figure 4. Profiles generated using Heaviside and Logistic functions (with radiation)....18

Figure 5. Profiles generated using Heaviside and Logistic functions (no radiation) 19

Figure 6. Welhead temperature with time 23

Figure 7. Temperature profiles during three drawdowns 24

Figure 8. Temperature profiles at different values of time during shut-in 25

Figure 9. Temperature vs. depth for various times 32

Figure 10. Temperature vs. depth for various flow rates at t = 0.5 hr.....34

Figure 11. Temperature vs. depth for various times at injection rate of 5760 BWPD.....35

Figure 12. Temperature vs. depth for various flow rates at t = 0.5 hr.....36

Figure 13. Temperature vs. depth for various injection temperatures.....38

Figure 14. Mud temperature vs. measured depth for different times (ε=0.2) 45

Figure 15. Mud temperature vs. measured depth for different times (ε=1) 46

Figure 16. Variation of temperature with radius at different values of time (ε=0.2) 47

Figure 17. Variation of temperature with radius at different values of time (ε=1) 48

Figure 18. Change in average tubing temperature over time for different values of ε.....49

Figure 19. Cross section of a multilayer concentric cylinder.....76

LIST OF TABLES

Page

Table 1 Input Parameters for the Production Example Case.....14

Table 2 Input Parameters for the Injection Example Case.....31

Table 3 Input Parameters for the Static Mud Example Case 43

CHAPTER I

INTRODUCTION

Many petroleum engineering problems require that transient temperature of wellbore fluid is known. This chapter introduces those problems. Details of how transient temperature can be of great significance for solving them will follow. Three major problems have been studied in this thesis.

Single and Transient Rate Production

Interest in transient temperature during production could be because of various reasons. Gas hydrate plugs can form in gas wells under certain pressure and temperature conditions. Similarly, for oil wells, wax can choke the wellbore during production when pressure and temperature are within certain range. Knowledge of temperature can help avoid such situations. Another application is pressure transient testing which will remain our focus to demonstrate capabilities of our transient temperature models for production case.

Pressure transient testing involves measurement of pressure by varying flow rates. There are many different types of pressure transient tests. These tests often involve measurement of either the flowing or shut-in downhole pressure. Many wells have permanent downhole gages that record pressure. However, there are many more wells where it is not economically feasible to install permanent downhole gages. Under such

circumstances bottomhole pressure can only be calculated using the measured wellhead pressure. During transient tests well is not in thermal equilibrium with the surroundings. Density of wellbore fluid varies with temperature which keeps on changing with time during the test. In order to determine accurate bottomhole pressure one needs to take into account the unsteady temperature changes in wellbore fluids.

Hasan et al. (2005) proposed a model to estimate transient temperatures during production and shut-in. However, the model assumes that variation of wellbore fluid temperature with depth (dT_f/dz) is time invariant. Spindler (2011) removed this assumption by solving their temperature distribution equation using method of characteristics, but doing so introduced a discontinuity in solution. However, fluid temperature profiles are rarely discontinuous. A model is presented in Chapter III of this thesis that calculates smooth temperature profile.

Pressure transient tests also involve series of dissimilar but constant flow rates. For instance, in a multirate test there are several drawdowns and buildups of equal time duration. A drawdown is followed by a buildup and alternate drawdowns and buildups are repeated several times to determine well deliverability. Another example of the rate change is the flow-after-flow test. During this test, well is flowed at a constant flow rate till the pressure response is stabilized. The flow rate is then increased and the well is flowed again at the new flow rate till the pressure response stabilizes again. This process is repeated three or four times. Thus, for such tests involving transient rates a model is

needed which could determine the transient temperature with changes in the flow rate. A model is presented in Chapter IV that is fully capable of calculating the transient temperature with change in flow rates.

Experience of modeling temperature for production case helped in design of temperature models for injection. This is because of similarity of production and injection operations in terms of physics and mathematical formulation. Injection is going to be the topic of our discussion in next section.

Single Rate Injection

Knowing wellbore fluid temperature with time is of importance in injection process. A major application where the knowledge of wellbore fluid temperature is critical is that of the acidizing treatment. Different kinds of acids are injected into the reservoir as part of production stimulation program. Properties of acids are dependent on temperature. Some acids become very corrosive for metal in the wellbore system if pumped at high temperatures. This necessitates cooling of wellbore system by injecting water before any acid is pumped downhole. Time and resources need to be determined for such kind of acid treatments. Another application is injection of hot oil for removal of paraffin wax in the tubulars. Wax gets deposited in the near wellbore region and the tubing over time during production. It is molten off the metal surface by exposing it to hot oil. Although there could be more applications of injection model that can be imagined only two are discussed here.

An attempt has been made to develop a model that can predict transient wellbore fluid temperature for fluid injection by modifying Hasan et al. (2005) temperature distribution equation. The details of the proposed model are in Chapter V. This section concludes our discussion of temperature models that are useful for calculating temperature profiles of either *flowing* or *static* wellbore fluid during production and injection operations.

Mud Temperature after Cessation of Circulation

Aforementioned models can be used for prediction of transient temperature for the flowing or static wellbore fluid. The model that is about to be discussed here is exclusively for determination of temperature for static fluid. Static borehole mud column is used as an example to demonstrate the functionality of our proposed model.

Lowering the temperature of the drill bit is one of the primary objectives of circulating mud through borehole. When mud circulation ceases, the temperature of *now-static* mud column would start to increase through heat transfer from the higher temperature formation. This temperature increase would change mud rheological properties adversely and may cause safety problems. Estimating time required for mud to heat up is important for preparation of standard operating procedures of workover or drilling operations. This problem has been modeled in Chapter VI as transient radial heat conduction in a multilayer cylinder.

Proposed Solutions

Solutions proposed in this work are summarized as follows:

1. Smooth semianalytical solution of Hasan et al. (2005) temperature distribution equation is presented.
2. A new purely analytical model for predicting transient temperature of wellbore fluid for situation involving transient rates during production is developed.
3. A new semianalytical model for calculation of transient temperature during injection operations is presented. Two additional equations can determine the time required to cool down the entire wellbore depth for acidizing treatment and the depth of effectiveness of paraffin wax removal treatment.
4. An analytical model for transient temperature of static borehole fluid column is derived.

CHAPTER II

LITERATURE REVIEW

Literature review was done for each of the three problems discussed in Introduction.

Single and Transient Rate Production

Kirkpatrick (1959) was one of the first to model temperature profiles. Ramey (1962) developed a theoretical solution for wellbore fluid temperature for single phase incompressible liquid or single phase ideal gas. Satter (1965) attempted to improve Ramey's model by incorporating effects of phase change in steam injection wells. Shiu and Beggs (1980) studied the data of 270 wells from three geographic locations and presented an empirical method for calculating wellbore fluid temperatures of two-phase flow wells. Sagar et al. (1991) incorporated effects of kinetic energy and Joule-Thomson expansion in their empirical model and proposed an improvement over Shiu and Beggs (1980) model. Alves et al. (1992) came up with a unified equation for flowing temperatures. Their model is applicable to pipelines and wellbores alike. They set up their solution in such a way that it degenerates into Ramey (1962) equation for single phase incompressible liquid or ideal gas and into the Coulter and Bardon (1979) equation for other case. Hasan and Kabir (1994) formulated a solution for flowing wellbore temperature which took wellbore as cylindrical source instead of a linear source as assumed by Ramey (1962). Their results showed excellent match with the field data when convective heat transfer in casing annulus was also included in heat transfer

calculations. Hagoort (2004) presented a graphical correlation to estimate the length of early transient period of flowing well and later presented an analytical solution for wellbore fluid temperature of gas wells (Hagoort 2005). In addition to their original model for single deviation wells, Hasan et al. (2009) also made a model for complex wells. Please note that all of the above models are for steady state flow.

This brings us to the transient temperature models. Hasan et al. (2005) devised a model for the transient wellbore fluid temperature which has two separate equations for drawn-down and buildup. They validated their model with the field data. Guo et al. (2006) designed a model for estimating temperature profiles in pipelines with different kinds of insulations. Guo et al. (2006) have considered conduction through the insulation as the only heat transfer mechanism while, in addition to conduction, model presented in this thesis takes into account, various other resistances to heat transfer in the wellbore, especially the natural convective heat transfer in the annulus fluid. Additionally, this model takes into account effects of Joule-Thomson expansion and thermal storage of wellbore system which are absent in Guo et al. (2006) model. Spindler (2011) solved the temperature distribution equation of Hasan et al. (2005) while incorporating the effects of longitudinal heat conduction along the wellbore. At the same time, Spindler (2011) acknowledges the fact that conduction doesn't have much of an impact on the wellbore temperature profile. In addition, the model is very unwieldy because of very lengthy equations which are apparently not improving the simpler model of the same paper. Several other models that take numerical approach exist to compute transient flowing

fluid temperature. However, we will focus only on analytical modeling here because of its ease of implementation and speed with which calculations can be done.

Single Rate Injection

Moss and White (1959) presented a steady state temperature model for injection. Their model had a constant-rate line source solution of diffusivity equation. So does the Ramey (1962) who also introduced overall heat transfer coefficient while modeling temperature of injection fluids. Squier et al. (1962) developed two solutions: one for short time and the other for steady state. Their model considers casing and cement zone as part of the formation. Eickmeier et al. (1970) presented a finite difference model for calculating transient temperature during production and injection. Arnold (1989) made an analytical model for hot liquid injection down the annulus of wellbore. Guo et al. (2004) presented a model for calculation of transient temperature for thermal injection lines. However, this model has limited applicability because it requires that the temperature of fluid at entry point should be same as the medium surrounding the entry point. Moreover this model doesn't take into account thermal storage of wellbore system and Joule Thomson effect.

Mud Temperature after Cessation of Circulation

Bulavin and Kashcheev (1965) presented a solution of heat conduction equation that was applicable to multilayer bodies including plates, cylinders and spheres. Singh and Jain (2008) presented a solution for transient heat conduction equation that was applicable

only for multilayer cylinders. There are several other authors who have studied the problem of multilayer bodies but above two are the most relevant for our case. A novel implementation of transient temperature solution of heat conduction through multilayer cylinder is presented in this thesis.

CHAPTER III

SINGLE RATE PRODUCTION

Introduction

Hasan et al. (2005) have demonstrated the use of their transient temperature model that employs an assumption which reduced the number of variables in their original differential equation from two to one. Goal of this chapter is to attempt to improve this model and then to develop solutions that could predict flowing wellbore fluid temperatures for other conditions. Please note that for the models presented in this chapter and the next one, the Hasan et al. (2005) temperature distribution equation has not been modified in any way. Rather, new solutions have been created by using the temperature distribution equation in its original form with new boundary and initial conditions.

Hasan et al. (2005) devised their model by applying energy balance for control volume within wellbore for two-phase fluid. Radial heat transfer between fluid and surrounding formation was modeled using an overall heat transfer coefficient which included thermal resistances for conduction due to tubing, insulation, casing and cement material. Forced convection due to tubing fluid and natural convection in the casing annulus was also taken into account.

Formation temperature distribution was modelled using heat diffusion equation where wellbore was modelled as finite cylindrical heat source. The principle of superposition was used to model the decrease of heat transfer from wellbore to formation over time. Their dimensionless temperature distribution solution had integrals of Bessel function so simpler algebraic approximation was used instead. Details are given in Hasan and Kabir (1991) and Hasan et al. (2005).

Hasan et al. (2005) developed the following expression for transient fluid temperature,

$$(1+C_T)\frac{\partial T_f}{\partial t}-\frac{w}{m}\frac{\partial T_f}{\partial z}=\frac{w}{m}L_R\left[T_{ei}(z)-T_f\right]+\frac{w}{m}\left(\phi-\frac{g\sin\alpha}{c_pJg_c}\right) \quad (1)$$

Following boundary and initial conditions were used:

Boundary condition:

$$T_f(L,t)=T_{eibh} \quad (2)$$

Initial condition:

$$T_f(z,0)=T_{eibh}-(L-z)g_G\sin\alpha \quad (3)$$

We have used Laplace transform to solve Eq. 1 with the boundary and initial conditions given by Eqs. 2 and 3 respectively. Solution to Eq. 1 is:

$$T_f=T_{ei}(z)+\frac{\psi}{L_R}\left[1-e^{-\frac{wL_R}{m(1+C_T)}t}-\left(e^{-(L-z)L_R}-e^{-\frac{wL_R}{m(1+C_T)}t}\right)H\langle x\rangle\right] \quad (4)$$

where H is the Heaviside function

$$H(x)=\begin{cases}0, & x\le 0\\ 1, & x>0\end{cases} \quad (5)$$

and

$$x = t - \frac{(1 + C_T)(L - z)}{\frac{w}{m}} \tag{6}$$

Spindler (2011) arrived at the same solution given in Eq. 4 however this solution causes discontinuity in wellbore temperature profile because of the step (Heaviside) function. Approximation of step function as follows removes the discontinuity:

$$T_f = T_{ei}(z) + \frac{\psi}{L_R}\left[1 - e^{-\frac{wL_R}{m(1+C_T)}t} - \left(e^{-(L-z)L_R} - e^{-\frac{wL_R}{m(1+C_T)}t}\right)\widehat{m}\right] \tag{7}$$

where

$$\widehat{m} = \begin{cases} 1 - \dfrac{1}{1 + \left(\dfrac{z}{z'_{prod}}\right)^{\hat{B}}}, & L > z'_{prod} > 0 \\ 1, & z'_{prod} = 0 \; or \; z'_{prod} \geq L \end{cases} \tag{8}$$

where

$$z'_{prod} = L - \frac{vt}{1 + C_T} \tag{9}$$

and

$$\hat{B} = \frac{4.59}{ln\left(\dfrac{L}{z'_{prod}}\right)} \tag{10}$$

Example Case and Discussion

Here we compare the temperature profiles found using our proposed model of Eq. 7 with those of Bahonar et al. (2011). The parameters required for the study are listed in Table 1 which are taken from Bahonar et al. (2011).

Fig. 1 compares the results of temperature profiles generated using Eq. 7 with those of Bahonar et al. (2011) for different times at a fixed flow rate.

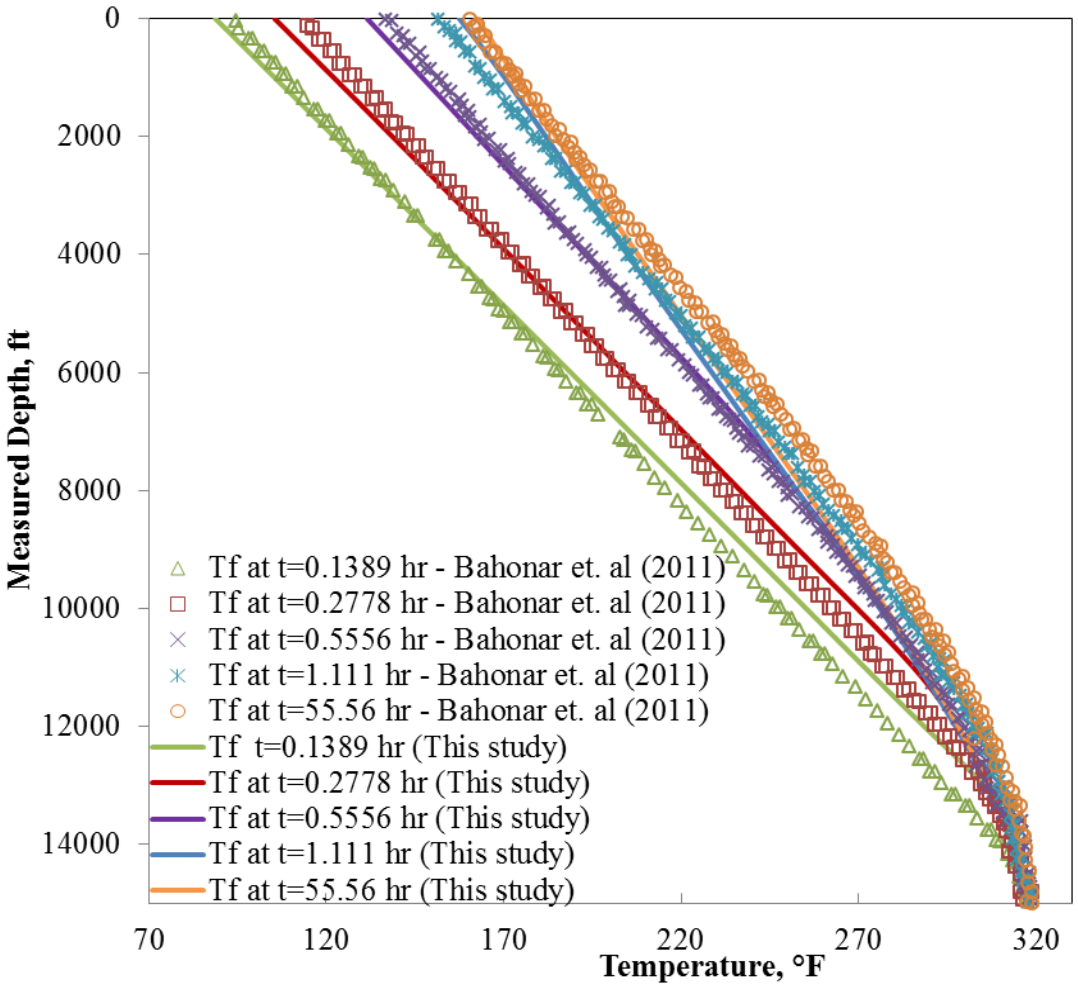

Fig. 1-Comparison of temperature profiles of Bahonar et. al (2011) and this study

Total Vertical Depth, ft	15000
Measured Depth, ft	15000
Inclination, degrees	90
Pipe Roughness, ft	0.00001
Tubing ID, in.	2 5/9
Tubing OD, in.	3 ½
Casing ID, in.	9
Casing OD, in.	10 ¾
Cement ID, in.	10 ¾
Cement OD, in.	16
Surface Temperature, °F	70
Bottomhole Temperature, °F	317.5
Coefficient of Thermal Expansion (β), 1/°F	0.00209
Critical Pressure, psia	675.43
Critical Temperature, °R	384.41
Specific gravity of gas	0.651
Thermal conductivity of tubing fluid, Btu/(hr-ft-°F)	0.018
Thermal conductivity of tubing, Btu/(hr-ft-°F)	25
Thermal conductivity of annulus fluid, Btu/(hr-ft-°F)	0.01671
Thermal conductivity of casing, Btu/(hr-ft-°F)	25
Thermal conductivity of cement, Btu/(hr-ft-°F)	1.15
Thermal conductivity of formation, Btu/(hr-ft-°F)	2
Emissivity of casing inside surface	0.9
Emissivity of tubing outside surface	0.9
Specific heat of gas, Btu/(lbm-°F)	0.514
Specific heat of annulus fluid, Btu/(lbm-°F)	0.241
Geothermal gradient, °F/ft	0.0165
Production rate, MMSCF/D	5
C_T, dimensionless	0 (0.5)

Table 1-Input Parameters for the Production Example Case

Markers in Fig. 1 represent the temperature profiles that were digitized from Bahonar et al. (2011) while the solid lines are the results of this study. Bahonar et al. (2011) use the same energy balance equation in their model as Hasan et al. (2005) which is the reason why the temperature profiles obtained using Eq.7 and Bahonar et al. (2011) model are very similar.

Fig. 2 compares the temperature profiles calculated using Hasan et al. (2005) and this study. The figure shows how the temperature profiles would look like when dT_f/dz term in Eq. 1 is taken as time-variant as opposed to Hasan et al. (2005) model which take the dT_f/dz term as time-invariant.

Overall heat transfer coefficient was calculated using conventional heat transfer equations which are also present in Willhite (1967). Z factor was calculated using the method of Dranchuk et al. (1973). Heat transfer coefficient because of natural convection in annulus was calculated using the Hasan and Kabir (1994) adaption of correlation of Dropkin and Somerscales (1965). 5% of the calculated value was used as the convective heat transfer coefficient in annulus for further calculations. Wellbore was assumed to be of constant cross section throughout the depth of well. Friction factor in tubing was calculated using equation presented by Chen (1979).

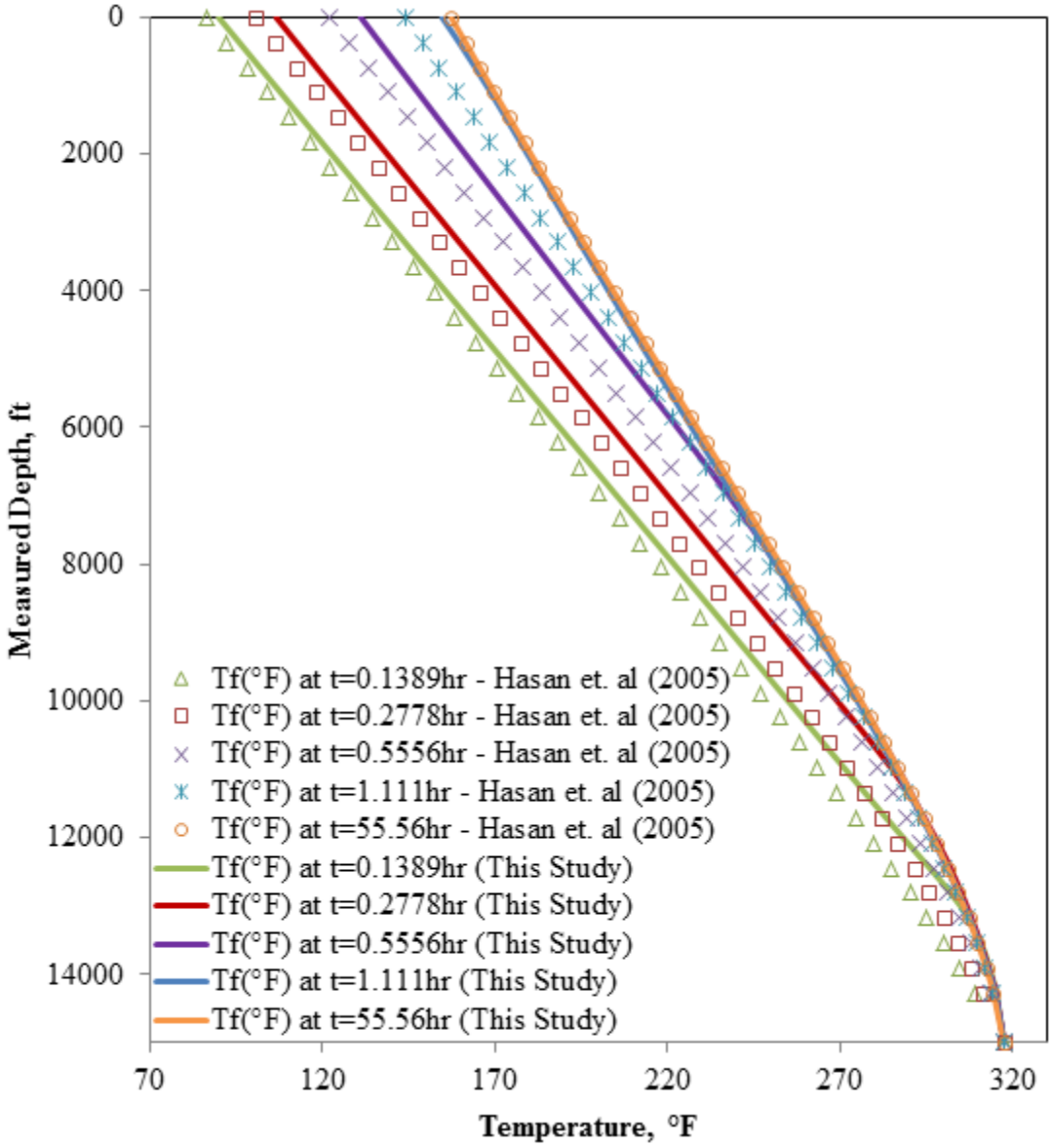

Fig. 2-Comparison of temperature profiles of Hasan et. al (2005) and this study

Input parameters listed in Table 1 are taken from the paper of Bahonar et al. (2011) while the values in small brackets are the values that were used to achieve a close match for temperature profiles with those of Bahonar et al. (2011).

The improvement in temperature profile is because of the Logistic function approximation of Heaviside function in Eq. **7**. Fig. 3 compares the Heaviside function and its approximation at t=0.2778 hr. Heaviside function is a step function. Its value can either be zero or one. It controls the speed of the temperature transient that passes through the wellbore. This is the reason why it causes a sharp discontinuity in the temperature profile. Logistic function on the other hand transitions smoothly.

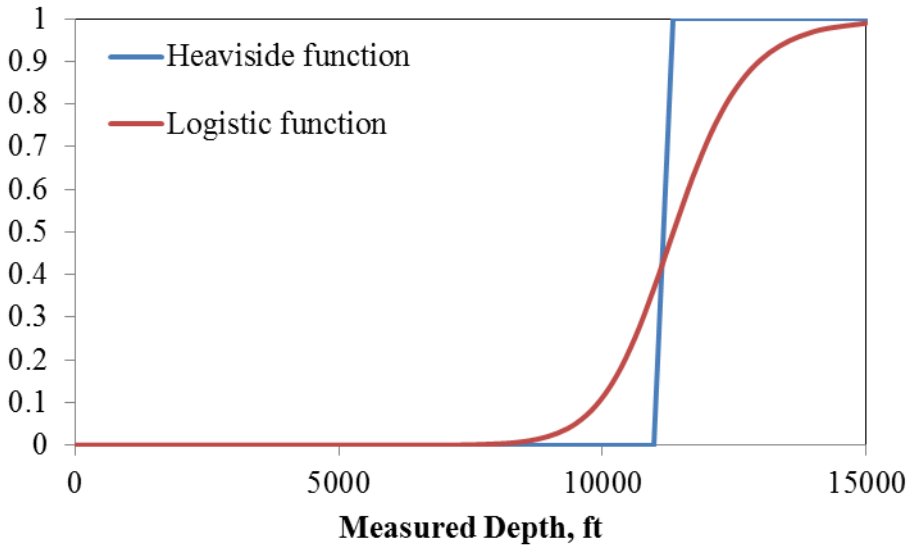

Fig. 3- Comparison of Logistic function and Heaviside function at t=0.2778 hr

Fig. 4 compares the temperature profile for the example case generated using the equation that uses Heaviside function as opposed to the equation that uses the Logistic function. Even though the difference between the profiles at 12000 foot depth is subtle, it can become more pronounced in certain cases. For example, if the effects of radiation

in annulus had been ignored (in case of low bottomhole temperatures or relatively shallow wells) the profile would make a very sharp turn at the same depth in case of Heaviside function as compared to Logistic function. (see Fig. 5)

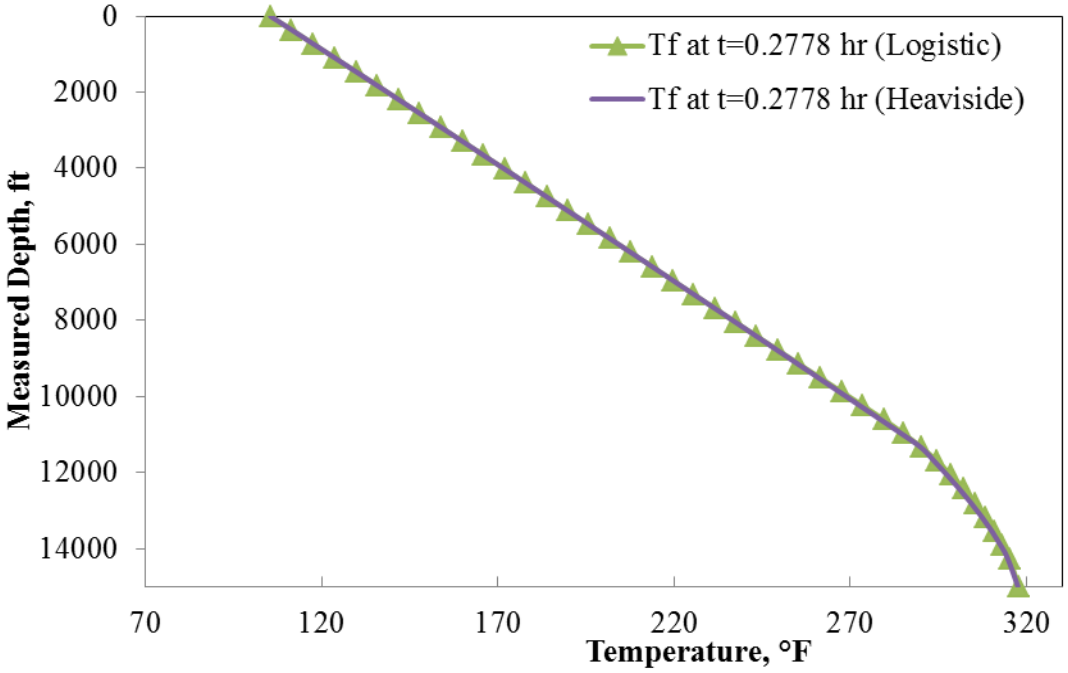

Fig. 4-Profiles generated using Heaviside and Logistic functions (with radiation)

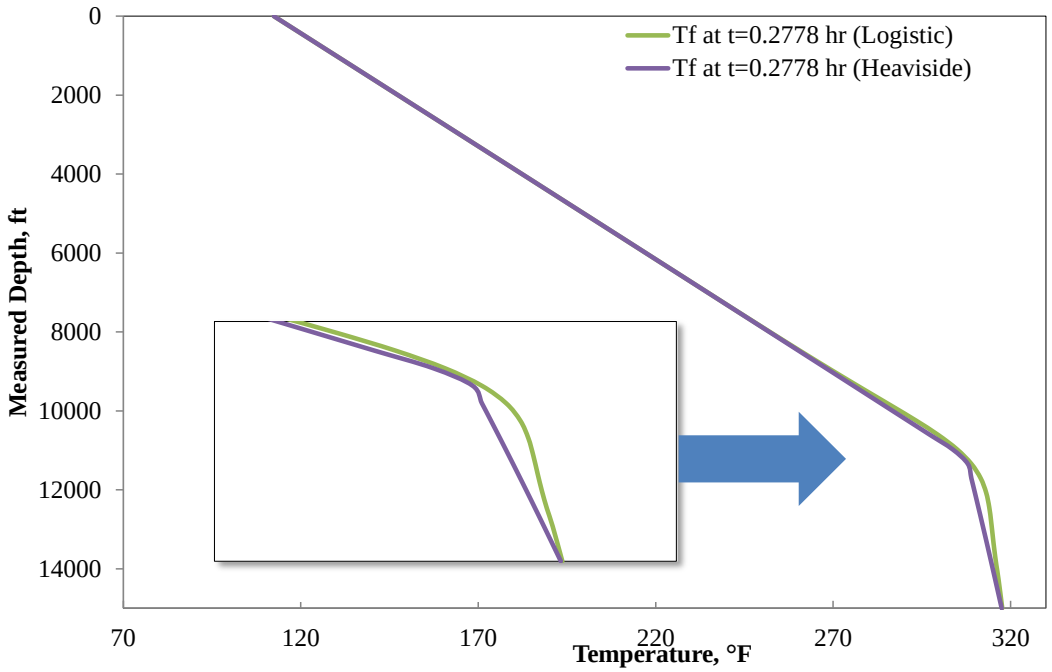

Fig. 5-Profiles generated using Heaviside and Logistic functions (no radiation)

Summary

Transient temperature distribution equation of Hasan et al. (2005) model was solved using the method of Laplace transform. The same equation has already been solved by Spindler (2011) using method of characteristics. However, Spindler (2011) solution has a disadvantage of discontinuity around the region given by Eq. 9.

The analytical method proposed in this chapter solved the problem of discontinuity by using Logistic function instead of Heaviside function. Since application of Laplace transform allows efficient solution of partial differential equations involving time, it will now be used to develop a model for a new flow configuration in next chapter.

CHAPTER IV

TRANSIENT RATE PRODUCTION

Introduction

The model presented in the last chapter works only for a *single* constant flow rate. However, actual wells are flowed at various constant flow rates. There are situations in which knowing the transient temperature of wellbore fluids is important while flow rate is being changed. Knowledge of temperature becomes important during the well deliverability tests. One such example is flow after flow test. In this test, well is flowed at a constant flow rate until the flowing pressure reaches a pseudo-steady state. Flow rate is then increased and well is flowed again till it achieves pseudo-steady state again. Change of flow rate is repeated three or four times. Multirate test presents another area where knowledge of temperature with transient rate becomes important. During a multirate test there are a series of drawdowns and buildups. Well is flowed at different rates during each drawdown. Once the temperature is calculated density can be calculated accurately which allows calculation of pressure. This model is useful in situations where permanent downhole gages are not present and only wellhead pressure has to be used to calculate the bottomhole pressure.

Eq. 1 can be solved for such a situation. Assume that well has flowed at a constant flow rate for a time after which the wellbore temperature profile has become steady. This is used as initial condition:

$$T_f(z,0) = T_f = T_{ei} + \frac{1 - e^{-(L-z)L_R}}{L_R}\psi \tag{11}$$

Using boundary condition given by Eq. 2, the solution to Eq. 1 is given by:

$$T_f = T_{ei}(z) + \frac{\psi'}{L'_R}\left(1 - e^{A't}\right) + \frac{\psi}{L_R}e^{A't}\left(1 - e^{-At-(L-z)L_R}\right) \tag{12}$$

for

$$H\left(t - \frac{m'}{w'}(1 + C_T)(L - z)\right) = 0 \tag{13}$$

and

$$T_f = T_{ei}(z) + \frac{\psi'}{L'_R}\left(1 - e^{-L'_R(L-z)}\right) \tag{14}$$

for

$$H\left(t - \frac{m'}{w'}(1 + C_T)(L - z)\right) = 1 \tag{15}$$

This model is fully capable of predicting temperature profiles for two cases:

1) Flow rate change
2) Well shut-in

Also notice that the solution given by Eqs. 12-15 is purely analytical in nature and approximations like Logistic function used in the model given by Eq. 7 have not been used here. There are two portions of the solution. Eq. 12 represents the transient portion of the solution. As time progresses, the solution degenerates into steady state equation represented by Eq. 14 here.

Example Case and Discussion

For the example case, well was flowed at successive flow rates of 5, 10 and 15 MMSCFD followed by a shut-in of 33 hours. Each drawdown lasted for 4 hours. Values listed in Table 1 are valid for this case unless otherwise stated in the body of this chapter.

Fig. 6 shows the variation of wellhead temperature with time. Please note that shut-in was simulated by using a very small flow rate of 500 SCFD instead of zero.

Fig. 7 shows wellbore fluid temperature profiles at various times during three drawdowns.

Here is how calculations were done: Fluid temperature for first drawdown was calculated using Eq. 7 of the last chapter. For the second and third drawdowns and subsequent shut-in, Eqs. 12-15 were used to calculate the transient temperature.

Overall heat transfer coefficient was calculated using the equations mentioned in Willhite (1967). Z-factor was calculated using the method of Dranchuk et al. (1973).

Natural convection heat transfer coefficient in annulus was calculated using the Hasan and Kabir (1994) adaption of Dropkin and Somerscales (1965) correlation. 5% of the calculated value was used as the convective heat transfer coefficient in annulus for further calculations. Wellbore was assumed to be of constant cross section throughout the depth of well. Properties like thermal conductivity, specific heat are assumed to be

constant. C_T value of 3 was used for the drawdown while for shut-in C_T was chosen to be zero.

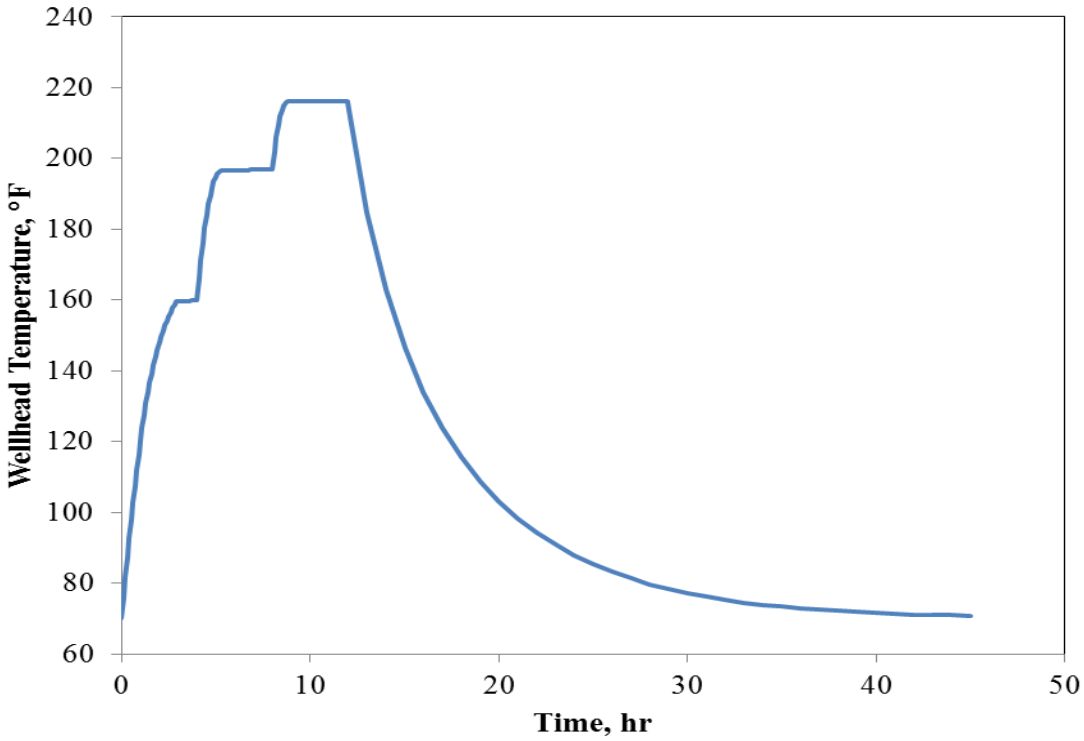

Fig. 6- Wellhead temperature with time

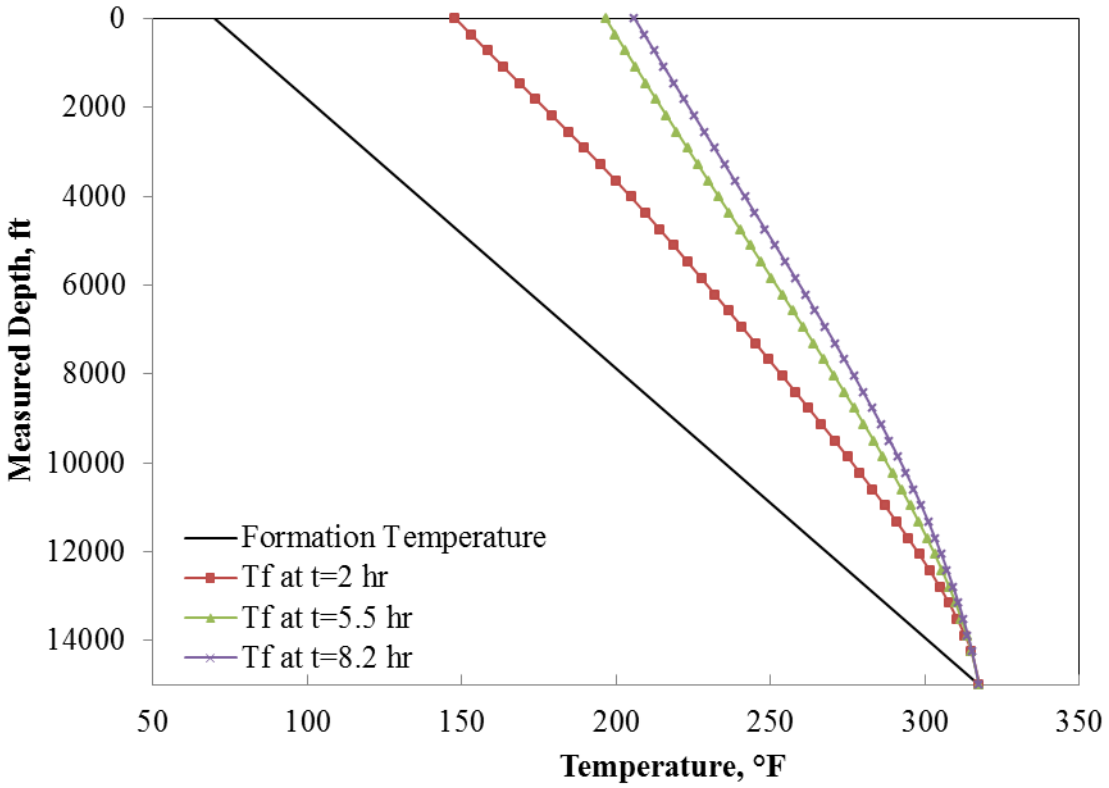

Fig. 7-Temperature profiles during three drawdowns

Fig. 8 shows temperature variation with time once the well is shut in. Observe that the temperature drops very rapidly right after the shut-in. This is because high temperature difference between the wellbore fluid and formation temperature causes heat transfer rate to be high initially. However as the time progresses the temperature difference decreases which reduces the speed with which temperature is dropping. Temperature matches the geothermal gradient at about t=45 hours.

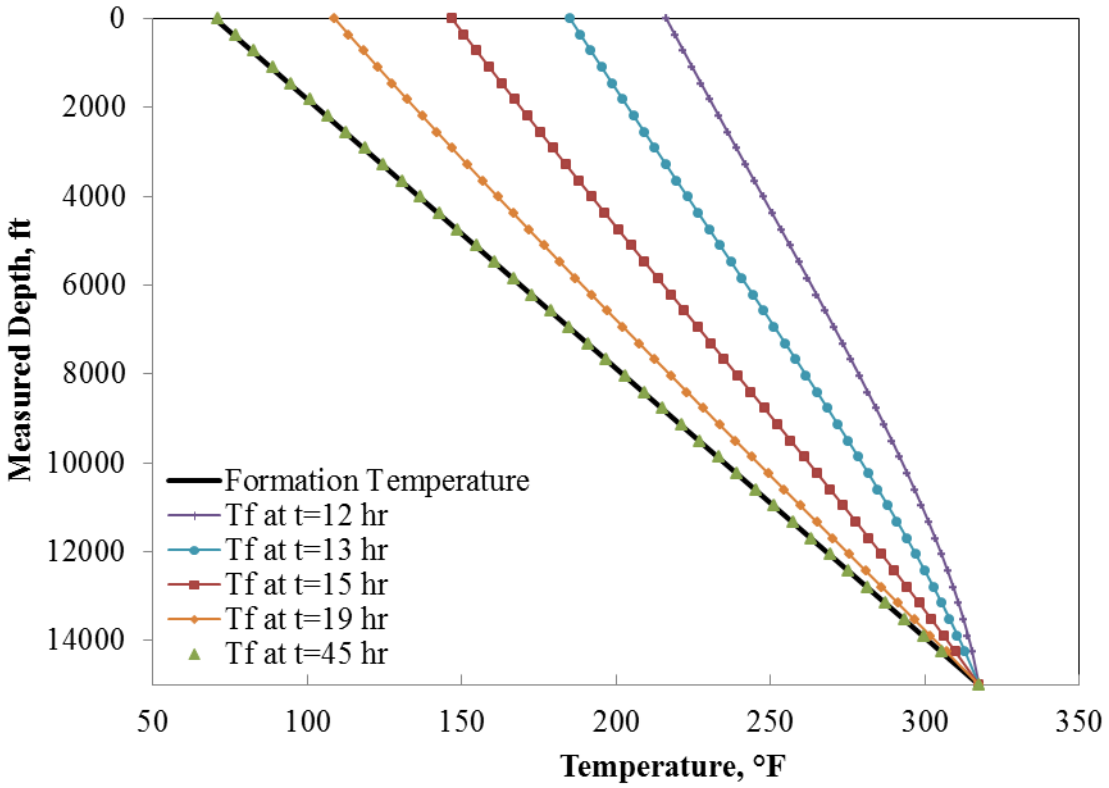

Fig. 8-Temperature profiles at different values of time during shut-in

Guo et al. (2006) have also developed a model for predicting temperature fluid in a pipeline after a rate change. However, they have considered conduction through the insulation as the only heat transfer mechanism while, in addition to conduction, our solution takes into account, various other resistances to heat transfer in the wellbore, especially the natural convective heat transfer in the annulus fluid. This model also takes into account effects of Joule-Thomson expansion and thermal storage of wellbore system which are absent in Guo et al. (2006) model.

Summary

Hasan et al. (2005) temperature distribution equation was solved with appropriate boundary and initial conditions to develop a new model for predicting wellbore fluid transient temperature after a change in flow rate. A synthetic case was used to demonstrate the functionality of the model. It can predict wellbore fluid transient temperature after a flow rate change and shut-in and is very useful in calculating temperature and pressure profiles iteratively during multirate and flow-after-flow tests.

Knowledge gained while making model for the production case has enabled us to implement same approach to model a physically and mathematically similar injection operations case in next chapter.

CHAPTER V

SINGLE RATE INJECTION

Introduction

Approach taken for the production case can also be applied to model transient temperature for injection operation. Transient temperature during injection is of interest due to several applications. Acid placement is one of those applications. Huenges and Ledru (2010) discuss how temperature can affect tubulars adversely during acid treatments. High acid temperature increases the rate of corrosion of tubing. High temperature can also reduce the efficiency of corrosion inhibitors. Knowing exactly how the temperature profile would look like with respect to time and depth would enable the designing of acid treatment in a much more efficient way. Pre-flushing the well with cold water would decrease the temperature of tubulars.

Model presented here would make it easy to take decisions regarding the type of acid used and/or how much water needs to be pumped into the reservoir to cool down the tubulars before final injection of acid can be done.

This leads us to another important application: wax removal treatment. Paraffin deposition in the tubulars and the near-wellbore region is a frequently-occurring problem in many oil fields. Hot oil is injected downhole to remove the paraffin in the tubing and near wellbore region. According to Straub et al. (1989), for rod pump systems heated

crude oil is pumped downhole to melt paraffin wax deposits periodically. The model presented here would also enable the user to gage the effectiveness of the treatment.

The temperature distribution model used for production in Hasan et al. (2005) model has been modified by only changing signs of terms for the case depicting the injection process as follows:

$$(1 + C_T)\frac{\partial T_f}{\partial t} + \frac{w}{m}\frac{\partial T_f}{\partial z} = \frac{w}{m}L_R\left[T_{ei}(z) - T_f\right] - \frac{w}{m}\left(\phi - \frac{g sin\alpha}{c_p J g_c}\right) \tag{16}$$

Eq. 16 is subject to following boundary and initial conditions:

$$T_f(0, t) = T_{fwh} \tag{17}$$

$$T_f(z, 0) = T_{sur} + z g_G \sin\alpha \tag{18}$$

Solution of Eq. 16 is given by:

$$T_f = T_{sur} + z g_G sin\alpha \; - \frac{\psi}{L_R}\left[1 - e^{-\frac{wL_R}{m(1+C_T)}t} + e^{-\frac{wL_R}{m(1+C_T)}t}\breve{m}\right] + \left(T_{fwh} - T_{sur} + \frac{\psi}{L_R}\right)e^{-zL_R}\breve{m} \tag{19}$$

$$\breve{m} = \begin{cases} 1 - \dfrac{1}{1 + \left(\dfrac{z}{z'_{inj}}\right)^{\breve{B}}}, & 0 < z'_{inj} < L \\ 1, & z'_{inj} = 0 \; or \; z'_{inj} \geq L \end{cases} \tag{20}$$

For acid treatment, time required to cool down the total depth of wellbore using water preflush is given by:

$$t_{cooling} = \frac{(1 + C_T)\,(L)}{\frac{w}{m}} \tag{21}$$

This is the time required by the temperature transient to reach bottomhole. At the value of time given by Eq. 21, wellbore temperature achieves pseudosteady state. At greater values of time the change of temperature with time is very small.

For hot oil treatment, the depth of effectiveness of treatment is given by the equation:

$$z_{effective} = \frac{1}{L_R} ln\left[\left(\frac{\psi}{L_R}\right)^{-1}\left(\frac{\psi}{L_R} + T_{fwh} - T_{sur}\right)\right] \quad (22)$$

It will be shown in the following section that for hot oil treatment the temperature of injected fluid is greater than the geothermal gradient till a certain depth at which the fluid temperature and formation temperature become equal. At depths below this point the temperature of injected fluid remains lower than the geothermal gradient. The crossover point between fluid temperature and the geothermal gradient marks the effective depth of the treatment. This depth was found by substituting formation temperature with the wellbore fluid temperature in Eq. A-48. Details of the derivation are in Appendix.

Example Case and Discussion

The proposed model has been used to calculate temperature profiles of water injection for the well described by the parameters listed in Table 2. Following assumptions were employed to obtain the results:

1. Heat conduction is ignored in vertical direction.
2. Heat transfer by radiation is ignored.

3. Wellbore heat capacities, thermal conductivities, wellbore thermal storage coefficient and density of annular fluid do not change with temperature.
4. Even though model is fully capable of handling Joule Thomson heating/cooling, it has been ignored for water injection.

A simulator was set up in MS Excel while iterations were performed using rudimentary VBA code. Wellbore was divided into 51 divisions of equal length with each division having same properties. Pressure drop, temperature and other properties were calculated for each division. Thermal resistances were calculated using conventional heat transfer analysis. Natural convection heat transfer coefficient in annulus was calculated using the Hasan and Kabir (1994) adaption of Dropkin and Somerscales (1965) correlation. 4% of the calculated value was used as the convective heat transfer coefficient in annulus for further calculations. Viscosity of water was calculated using Kestin et al. (1978) correlation.

Total Vertical Depth, ft	10000
Measured Depth, ft	10000
Inclination, degrees	90
Pipe Roughness, ft	0.0001
Tubing ID, in.	2.28
Tubing OD, in.	2.88
Casing ID, in.	5.012
Casing OD, in.	5.5
Cement ID, in.	5.5
Cement OD, in.	7.8
Wellhead Pressure, psia	8000
Wellhead Temperature, °F	50
Surface Temperature, °F	50
Coefficient of Thermal Expansion (β), 1/°F	0.0021
Thermal conductivity of tubing fluid, Btu/(hr-ft-°F)	0.2
Thermal conductivity of tubing, Btu/(hr-ft-°F)	25
Thermal conductivity of annulus fluid, Btu/(hr-ft-°F)	2.1
Thermal conductivity of casing, Btu/(hr-ft-°F)	25
Thermal conductivity of cement, Btu/(hr-ft-°F)	0.5
Thermal conductivity of formation, Btu/(hr-ft-°F)	1.4
Specific heat of oil, Btu/(lbm-°F)	0.53
Specific heat of water, Btu/(lbm-°F)	1
Specific heat of annulus fluid, Btu/(lbm-°F)	1
Geothermal gradient, °F/ft	0.016
C_T, dimensionless	5

Table 2-Input Parameters for the Injection Example Case

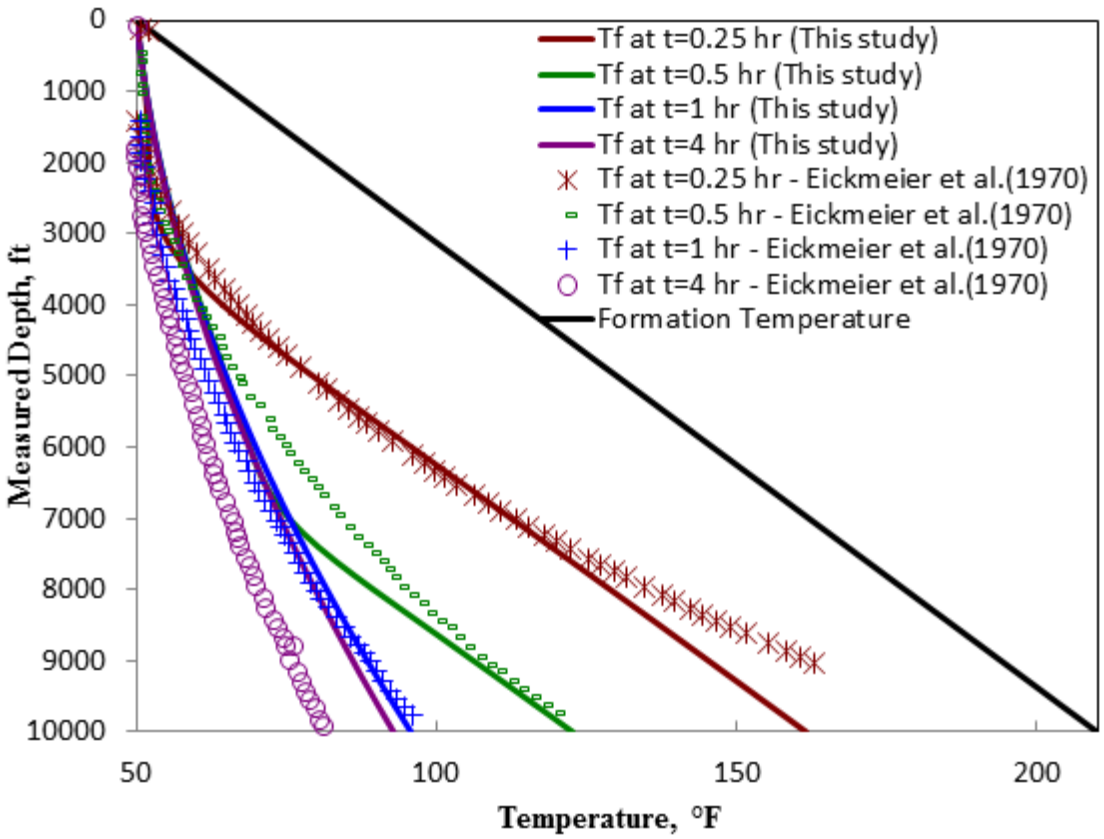

Fig. 9-Temperature vs. depth for various times

Fig. 9 gives the comparison of temperatures predicted by this study with those predicted by Eickmeier et al. (1970) for flow rate of 5760 BWPD at 0.25, 0.5, 1 and 4 hours.

Fig. 10 compares results of this study with the Eickmeier et al. (1970) for flow rates of 2880 BWPD, 5760 BWPD and 14400 BWPD at the injection time of 30 minutes.

Markers in Figs. 9-10 are the temperature profiles digitized from Eickmeier et al. (1970).

Obtained temperature profiles are intuitive. As water goes down the wellbore it starts to heat up. Since temperature difference between the injected fluid and formation is high at the start of injection, water experiences large increase in temperature. For the initial few thousand feet the temperature increases slowly but as water goes deeper in the wellbore the temperature goes up rapidly and the temperature profile becomes parallel to the geothermal gradient. Well starts to cool down. After a certain time (depending on flow rate) the temperature profile achieves pseudo-steady state and the change in temperature with time becomes extremely slow.

Results show a good match with Eickmeier et al. (1970) however model presented here has several advantages. Semianalytic nature makes this model much easier to implement using spreadsheets than the purely numerical model of Eickmeier et al. (1970). Moreover, since Hasan et al. (2005) temperature distribution equation, i.e. Eq. 16, has Joule Thomson term in it, temperature profiles for gas injection can also be calculated accurately. Also, Eickmeier et al. (1970) use a constant convective heat transfer coefficient for annulus fluids throughout the depth of the wellbore while for this study, heat transfer coefficient varies with depth and is therefore more representative of actual physical conditions.

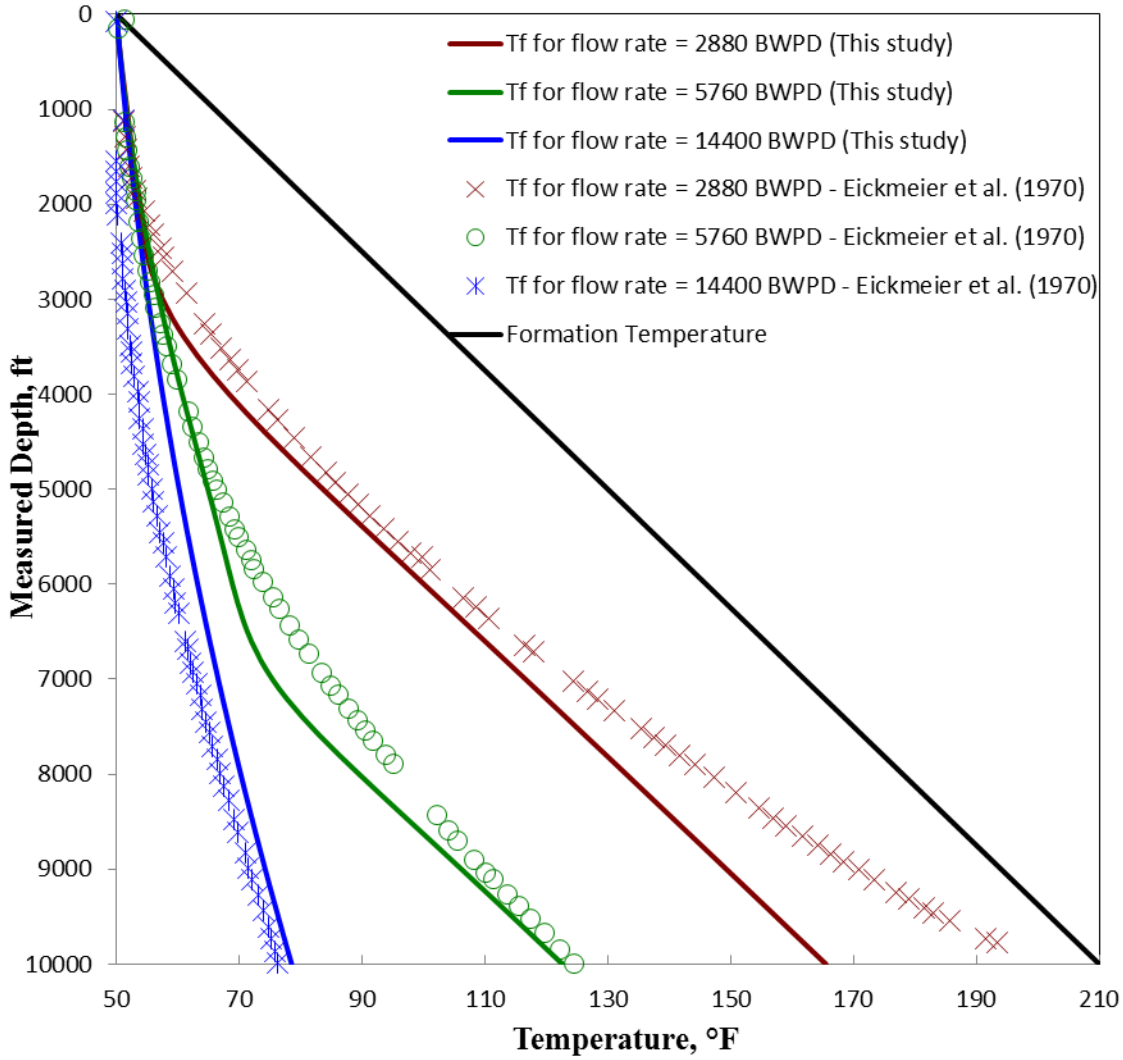

Fig. 10-Temperature vs. depth for various flow rates at t = 0.5 hr

The model was also used to calculate the temperature profiles for hot water injection for the same well. Input parameters listed in Table 2, except injection temperature, are valid for the temperature profiles shown in Figs. 11 and 12. Injection temperature is 70°F for both figures.

It is interesting to observe that for about first thousand feet the temperature of injected water is higher than the geothermal gradient until it becomes equal to the formation temperature. At deeper depths fluid temperature remains lower than the geothermal gradient.

Fig. 11 shows temperature transient passing through the wellbore system. At 0.25 hr the transient is at a shallow depth (see the "bulge" in maroon temperature profile). As the time passes the transient has reached deeper towards the bottomhole at 0.5 hr. The transient has passed completely through the system and temperature has achieved pseudosteady state at about 1 hr.

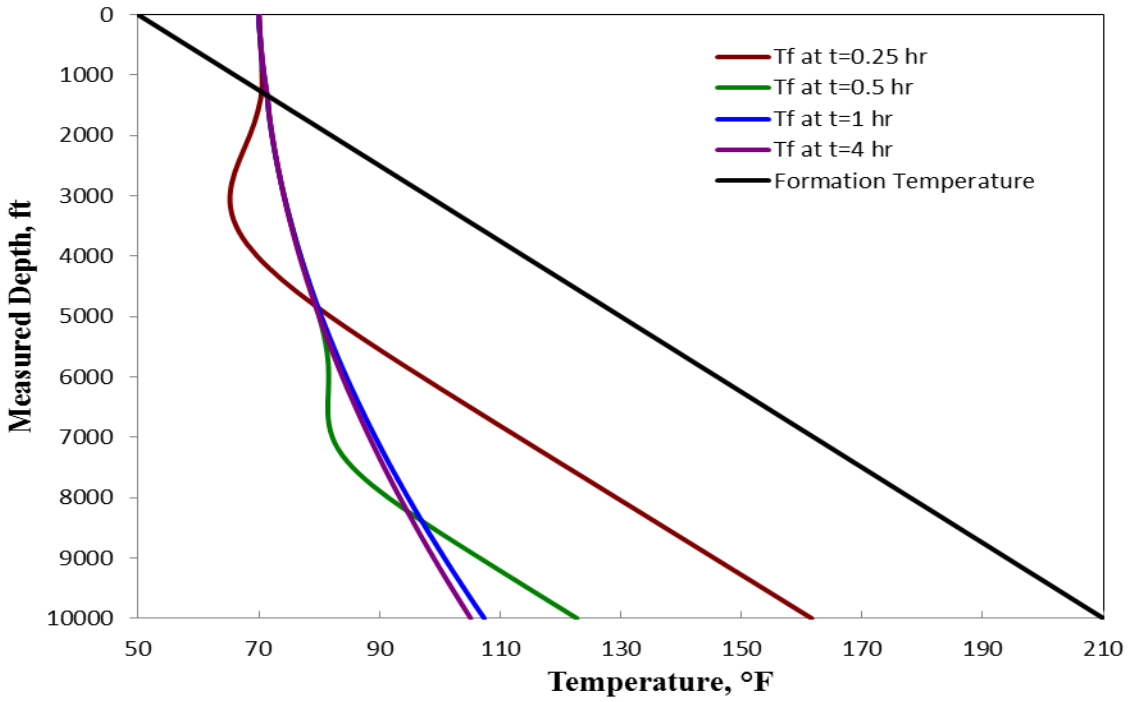

Fig. 11-Temperature vs. depth for various times at injection rate of 5760 BWPD

Physically this can be explained as follows: Before the injection is started, the fluid in wellbore is at rest and its temperature is same as the formation temperature. As the fluid is injected into the wellbore at a constant temperature it displaces the fluid originally present in the wellbore. The injection causes the temperature of fluid in shallower depths to achieve pseudosteady state faster while the temperature of the displaced fluid follows the same slope as the geothermal gradient. The "bulge" in the temperature profile represents the transient front where the injected fluid meets the displaced fluid that was originally present in the wellbore.

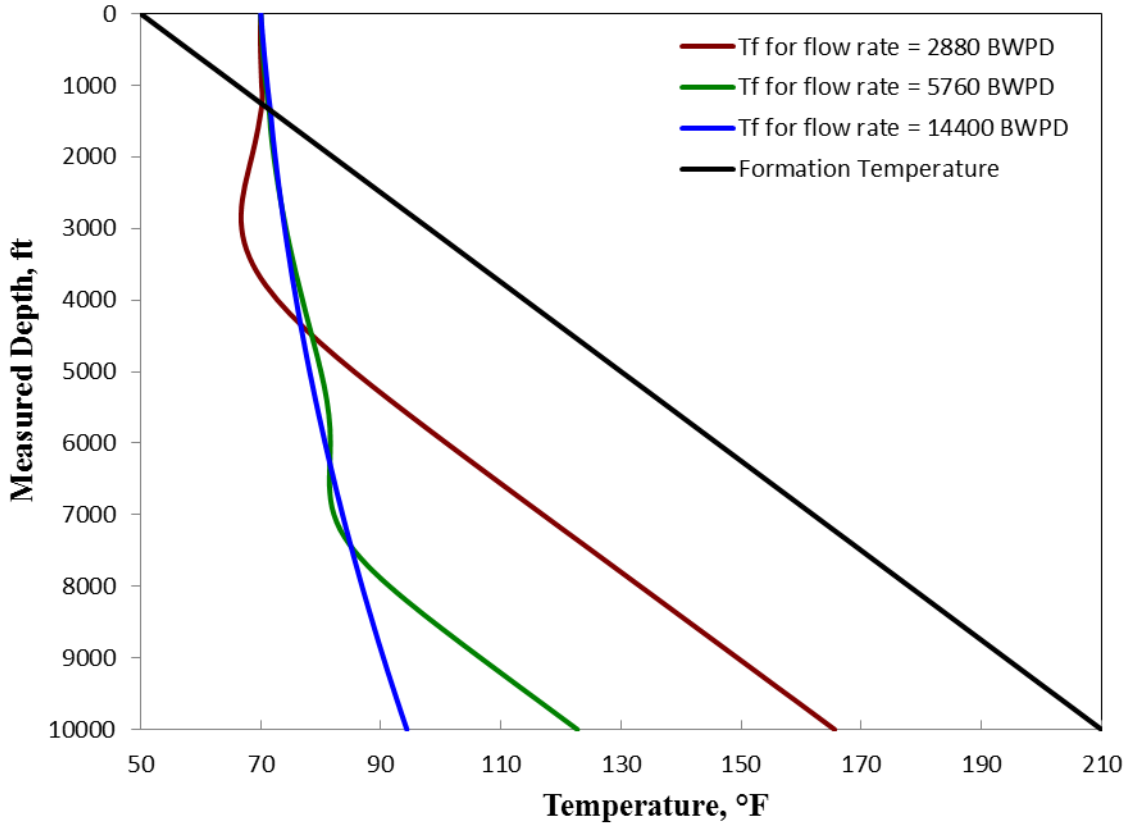

Fig. 12-Temperature vs. depth for various flow rates at t = 0.5 hr

If hot fluid is being injected to melt paraffin wax in tubulars, the effectiveness of treatment would be limited to the depth, given by Eq. 22 where injected fluid temperature becomes equal to the geothermal gradient. This is because at deeper depths the injected fluid temperature will be much lower than the geothermal gradient. Any wax deposited beyond that depth would remain solid. This point is made clearer in Fig. 13 which shows temperature profiles for various injection temperatures at injection rate of 5760 BWPD. For injection temperature of 70°F the depth till which fluid temperature is higher than the geothermal gradient is 1400 ft. When injection temperature is increased to 100°F this depth is increased to 3200 ft. This means that increasing injection temperature by 30°F has increased the depth, till which injection treatment will be effective, by 1800 ft in this case.

This depth can be further increased if tubing insulation is enhanced. Fig. 13 also shows that the model can predict temperature profile for injection temperature lower than the surface temperature. Time required to cool the entire wellbore depth can be calculated using Eq. 21.

Please note that Squier et al. (1962) presented a short-time solution and a long time approximation for hot water injection. However their model ignores the presence of casing and cement zone. They consider the casing and cement zone as part of the formation.

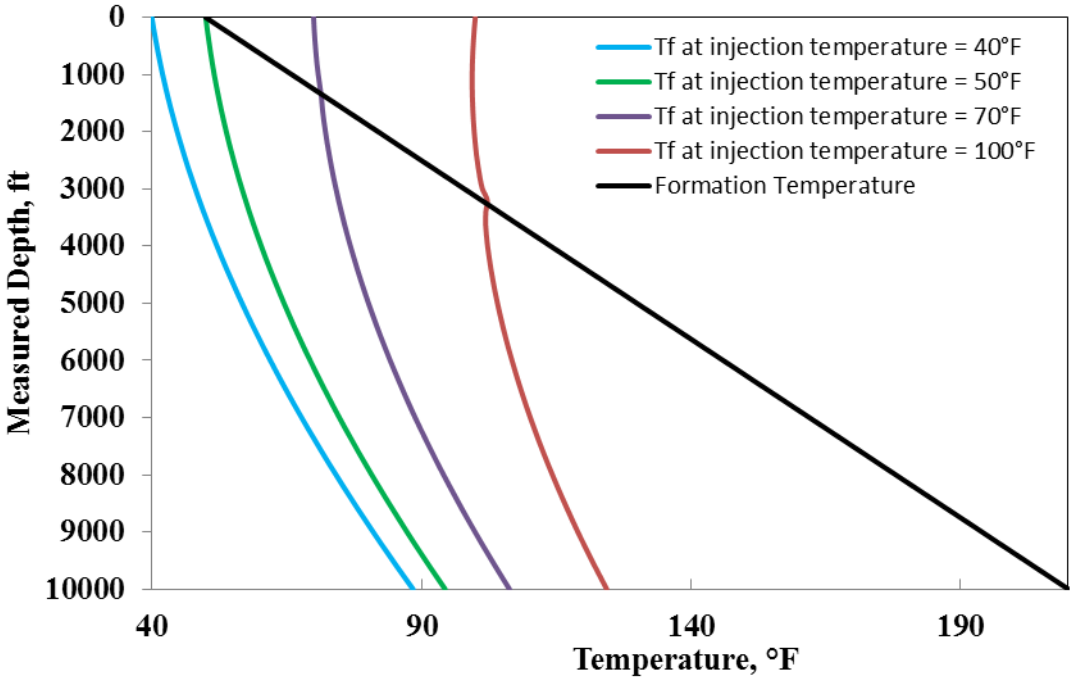

Fig. 13-Temperature vs. depth for various injection temperatures

Summary

Hasan et al. (2005) temperature distribution equation was adapted for the case of fluid injection and solved using Laplace transform to create a model for prediction of temperatures of injected fluids. Model accounts for Joule Thomson expansion and is therefore capable of predicting accurate gas injection temperatures also. Since model takes into account the surface injection temperature it can be used to plan acid treatments as well as treatments for removal of paraffin wax that involve injection of hot fluids. Two additional equations can predict the time required to cool the entire depth of wellbore, in case of acidizing treatment and the effective depth for paraffin wax removal

treatment respectively. Equations presented in this chapter are simple enough to be used with any spreadsheet software.

This chapter concludes the effort that was put in to model transient temperature for *flowing* wellbore fluids under different flow configurations. Details of how static borehole fluid temperature was modeled are presented in the next chapter.

CHAPTER VI

TRANSIENT TEMPERATURE OF STATIC MUD AFTER CESSATION OF CIRCULATION

Introduction

Although the model presented here exclusively calculates transient temperature of static fluid column, a brief overview of a preceding flowing condition is necessary for our discussion. Flowing mud temperature is of great interest because of numerous reasons. Maury and Guenot (1995) have discussed the advantages of cooling drilling mud. Mud returning from downhole needs to be cooled down before it is pumped back in order to maintain bottomhole at a temperature cooler than the geothermal temperature at that depth. MWD and LWD tools can only operate within a certain temperature range and it becomes absolutely necessary to cool down the bottomhole before MWD/LWD tools can be used. In case of oil-base muds, temperature of return flow should not be higher than the flash point so that it doesn't catch fire on the surface. Rheological properties of mud are temperature-dependent. In order for mud to perform its desired task, it has to be flowed at a temperature usually much cooler than the bottomhole temperature.

There are several models available that can predict the flowing mud temperature for mud flow in through annulus and out through tubing and vice versa. However, it is also necessary for the mud temperature to be determined once the flow *stops*. The model presented here can be used to determine the amount of time it would take for the mud to

heat up. This would help in estimating the amount of time driller has, to take corrective actions to re-establish flow in case of unplanned cessation of flow.

The heating/cooling of the wellbore mud has been modeled as a conduction problem of a multilayer cylinder. Following assumptions have been made:

1. Thermal properties do not vary with temperature.
2. No natural convection is taking place within borehole.
3. There is no heat conduction within the mud column in the longitudinal direction.
4. Formation temperature is assumed to be constant and follows a geothermal gradient.
5. The cross section of the hole is constant throughout the depth of hole.
6. Even though presence of mudcake buildup can be modeled using this model, here it has been neglected for the sake of simplicity.

Transient heat conduction equation in cylindrical coordinates is given by:

$$\frac{\partial^2 T_i}{\partial r^2} + \frac{1}{r}\frac{\partial T_i}{\partial r} - \frac{1}{\alpha_i}\frac{\partial T_i}{\partial t} = 0 \qquad (23)$$

Steady state temperature calculated using Kabir et al. (1996) model was used as initial condition while formation temperature was used as the outside boundary condition. Details of the interfacial conditions and solution are in Appendix.

Solution of transient heat conduction equation is:

$$T_i = T_{ei} + \sum_{n=1}^{\infty} a_n \, e^{-\alpha_i \lambda_{in}^2 t} R_{in}(\lambda_{in} r) \tag{24}$$

where a_n and R_n are given by:

$$a_n = \frac{\sum_{i=1}^{k} \frac{k_{eff,i}}{\alpha_i} \int_{r_{i-1}}^{r_i} r X_i R_{in} dr}{\sum_{i=1}^{k} \frac{k_{eff,i}}{\alpha_i} \int_{r_{i-1}}^{r_i} r R_{in}^2 dr} \tag{25}$$

$$R_{in}(r) = a_{in} J_0(\lambda_{in} r_i) + b_{in} Y_0(\lambda_{in} r) \tag{26}$$

$$k_{eff} = \epsilon k_{actual} \tag{27}$$

Analytical solution for conduction in multi-layer cylinder have already been published in literature like those of Bulavin and Kashcheev (1965) and Singh and Jain (2008), however such solution has never been applied or adapted to the borehole mud temperature calculation, to the best of author's knowledge.

Example Case and Discussion

Consider a borehole, described by parameters listed in Table 3, in which mud has flowed for 44 hours. At this point in time the temperature for the mud flowing through annulus and tubing has achieved pseudosteady state that has been calculated using Kabir et al. (1996) model. At the end of 44th hour the mud flow stops. This is exactly the time after which the model given by Eqs. 24-27 is used to calculate transient temperature of the borehole mud.

Total Vertical Depth, ft	15000
Measured Depth, ft	15000
Inclination, degrees	90
Drillstem OD, in.	6.625
Drill-bit size, in.	8.375
Mud Inlet Temperature, °F	75
Surface Temperature, °F	59.5
Thermal conductivity of mud, Btu/(hr-ft-°F)	1
Thermal conductivity of formation, Btu/(hr-ft-°F)	1.3
Thermal conductivity of formation, Btu/(hr-ft-°F)	1.3
Specific heat of mud, Btu/(lbm-°F)	0.4
Specific heat of formation, Btu/(lbm-°F)	0.2
Density of mud, ppg	10
Density of formation, lbm/ft^3	165
Geothermal gradient, °F/ft	0.0127
Viscosity of mud, lbm/ft.hr	110
Circulation rate, bbl/hr	300

Table 3-Input Parameters for the Static Mud Example Case

Formation temperature is assumed to vary linearly with depth. It is also assumed that at the borehole mud - borehole wall interface the temperature remains constant and equal to the formation static temperature. Flowing mud temperature given by Kabir et al. (1996) model was used as initial condition for the proposed model.

Note that Eq. 23 is a radial conduction equation. This means that it can determine the temperature variation with respect to time in radial direction only. In order to use it for this example, borehole was divided into 50 segments of equal length and temperature was assumed to be same throughout the depth of each segment. Interfacial contact

resistance between borehole wall and the mud plays a very important role. Mud cake buildup, along with rough borehole wall surfaces mean that heat transfer would not be perfect. This was modeled by using the concept of effective thermal conductivity. ε is used as a multiplier for thermal conductivity of mud. ε = 1 means that perfect thermal contact exists between the borehole mud and borehole wall interface. However, there would always be a thermal contact resistance at the interface because of roughness of borehole wall and presence of mudcake. To mimic such contact resistance a value of ε < 1 can be used. Model was used to predict the most conservative case of ε = 1 down to the best case scenario of ε=0.2. Latter is considered best case scenario because very small value of ε means mud would not heat up rapidly and thus would have better chance of avoiding deterioration of its properties.

Figs. 14-15 show the temperature profile of tubing mud at various values of time for the values of ε=0.2 and ε=1. Steady state temperature profile achieved after 44 hours of flow is represented by t=0 here. Observe that mud temperature is higher than the geothermal gradient for the upper portion of borehole until it crosses the geothermal gradient at a depth of around 8000 ft and becomes cooler in the lower half of the borehole. Cooler temperatures near the bottomhole are desirable so that MWD/LWD tools can be used safely. Moreover, mud rheological properties deteriorate if the mud heats up to the geothermal gradient at the bottom half of the well depth. For the case of high interfacial contact resistance, the well heats up much slower than the perfect contact assumption case.

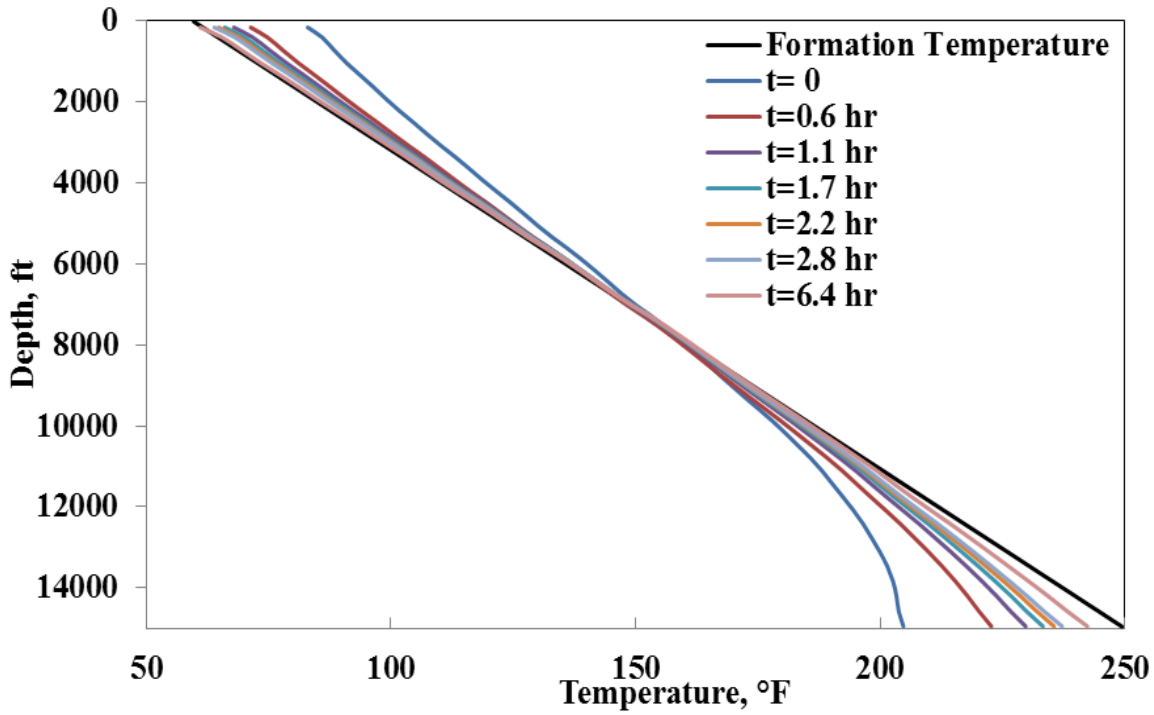

Fig. 14- Mud temperature vs. measured depth for different times (ε=0.2)

Knowing how fast or slow the mud heats up near the bottomhole is important because if for any reason the mud circulation stops, corrective measures could be taken. This model gives the time window driller would have to prevent mud properties from deteriorating.

Fig. 16 shows the variation of temperature with radius within tubing and annulus at different values of time for ε=0.2 near bottomhole where formation temperature is 245 °F. Once the flow stops, mud starts to heat up until its temperature becomes equal to the formation temperature in about 17 hours. For the same depth, mud heats up much rapidly if perfect thermal contact is assumed at the interface.

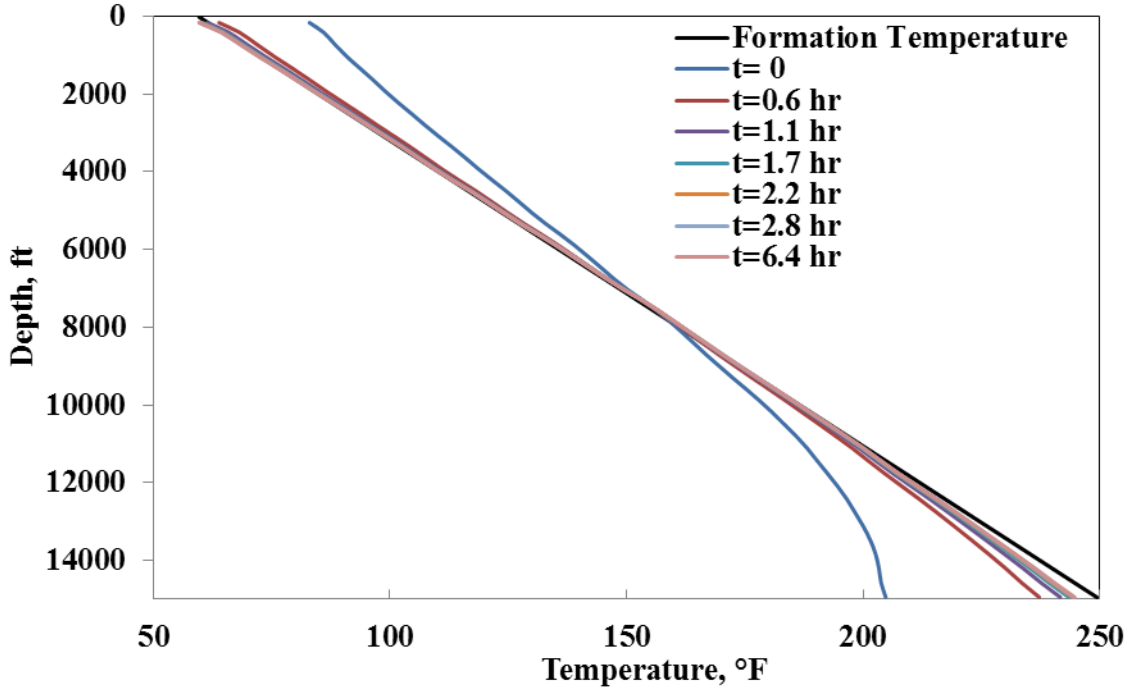

Fig. 15-Mud temperature vs. measured depth for different times (ε=1)

Fig. 17 shows that in a little over 2 hours mud heats up to the formation temperature.

Since comparison has been made, in the foregoing, between two extreme values of ε, it is now appropriate to show how temperature would vary for the intermediate values of ε.

Fig. 18 shows the variation of average tubing mud temperature with time. As the value of ε decreases from 1 to 0.2, the heat-up time of tubing mud increases.

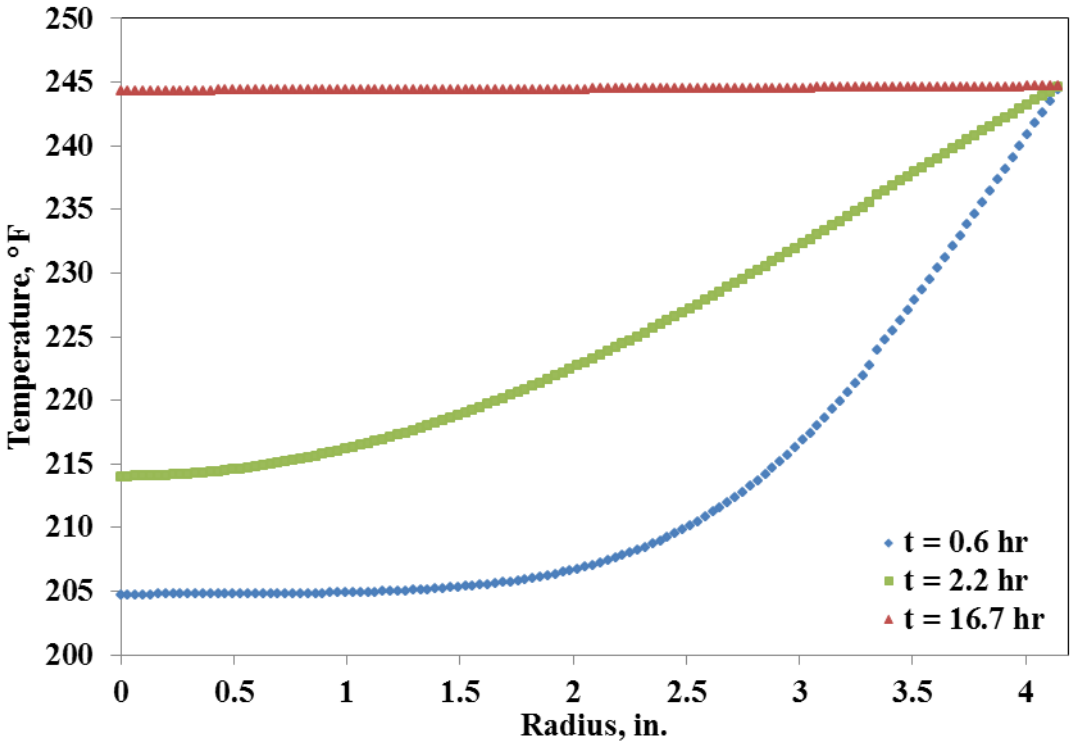

Fig. 16-Variation of temperature with radius at different values of time (ε=0.2)

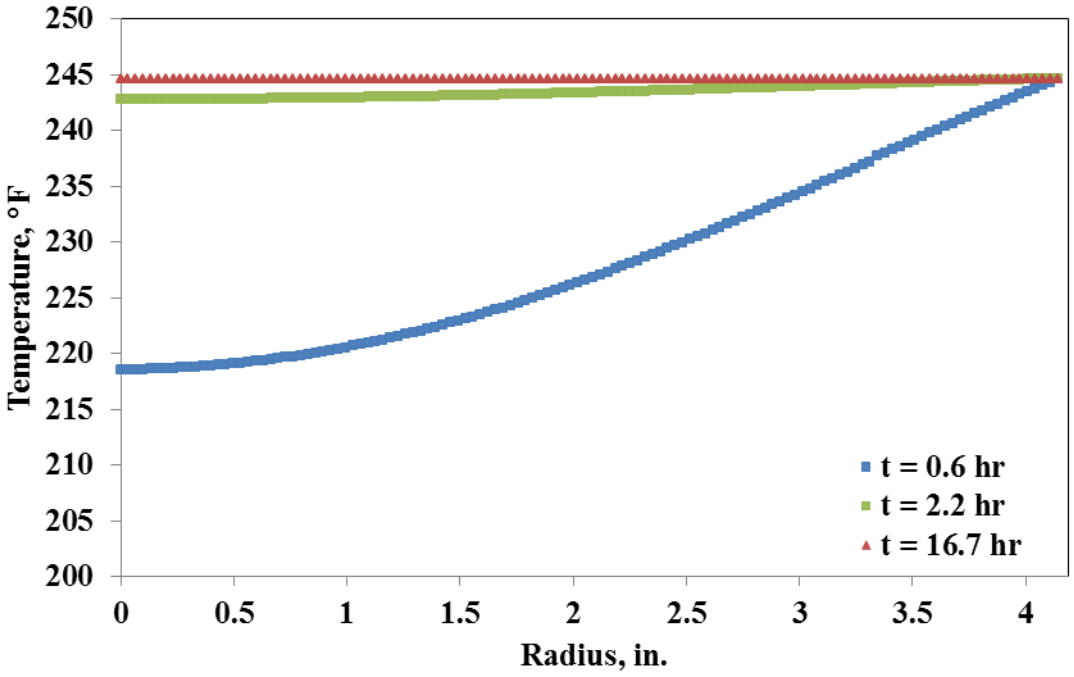

Fig. 17-Variation of temperature with radius at different values of time (ε=1)

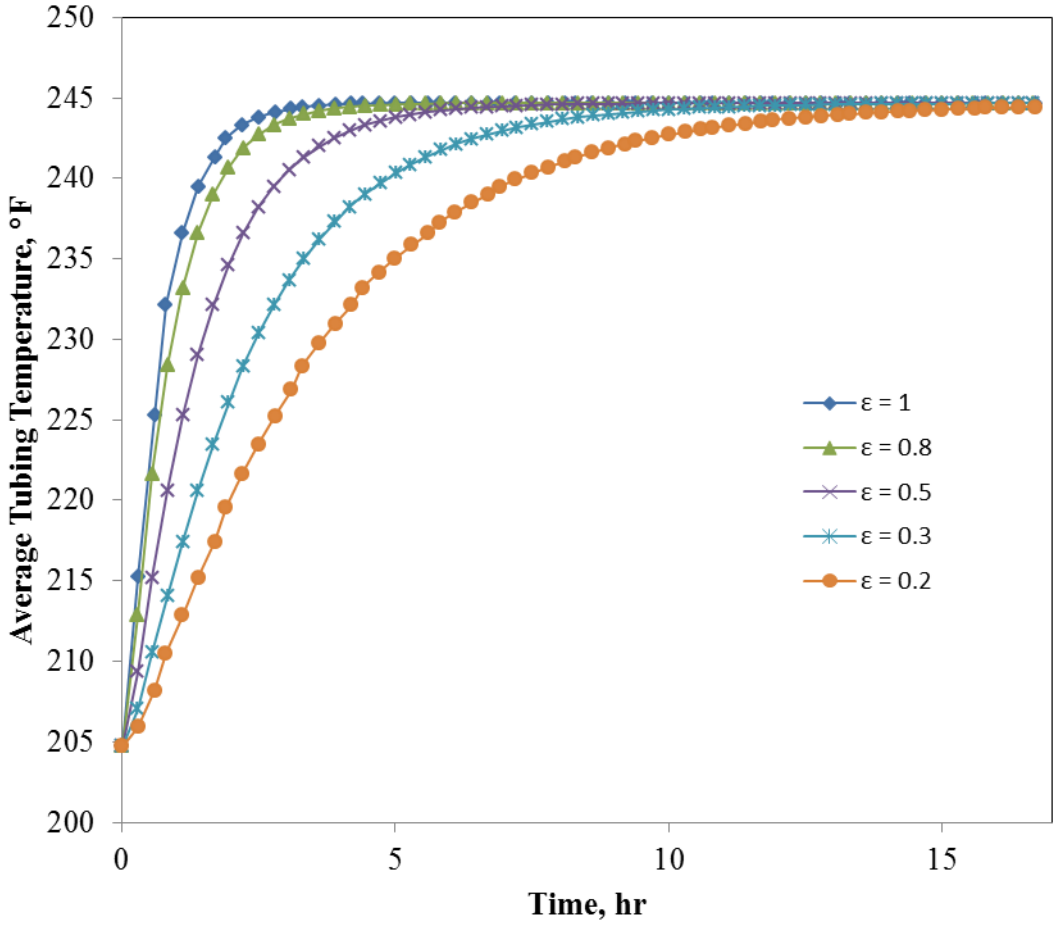

Fig. 18-Change in average tubing temperature over time for different values of ε.

Summary

Knowledge of borehole mud temperature is important because temperature has strong implications on mud rheology, operational safety, use of MWD/LWD tools. Transient radial heat conduction equation has been solved for appropriate initial and boundary conditions to develop a model for predicting transient temperature of drilling mud column upon accidental interruption of flow during drilling, work-over or completions operation. Mud column in tubing and annulus was modelled as a multi-layer cylinder

conduction problem. Concept of effective thermal conductivity has been used to model thermal contact resistance between borehole mud and borehole wall. Mud temperature profiles have been plotted for different values of depths, radius and time.

This chapter marks the end of the problems studied in this thesis. A final chapter that summarizes all that has been done so far is in order.

CHAPTER VII

SUMMARY

Thesis begins with the introduction of multiple problems for which transient temperature is important followed by the work that has already been done on the topics discussed in this thesis. Details of the problems are in separate chapters. Third chapter deals with the approximation of transient temperature solution of Hasan et al. (2005) done by Spindler (2011). Logistic function approximation of Heaviside step function has been used to smooth the solution. But this solution was only applicable for a single flow rate situation.

A model was then created to calculate transient temperature of wellbore fluids for multiple constant flow rates. Pressure transient testing was used as an example application for this model. Pressure transient testing requires accurate measurement of flowing pressure. Accurate prediction of downhole temperature is necessary in order to determine flowing pressure because density of wellbore fluids, especially gases, is dependent on temperature. During the test, fluid temperature keeps on changing with time because well has still not achieved thermal equilibrium with the surrounding formation. This is exactly the reason why we need a model to predict temperature with time. The model becomes very useful when only wellhead conditions are known and bottomhole pressure has to be determined using the wellhead pressure. Multirate tests and flow-after-flow tests are two of the various pressure transient tests that involve flow

rate changes. A model for predicting transient temperature for transient rates was developed by solving Hasan et al. (2005) temperature distribution equation. Steady state temperature equation was used as initial condition for this solution. The model's functionality was shown using a synthetic case.

Fifth chapter introduces the reader to the transient temperature modeling of injection fluids. This is important for various reasons including acid treatments and paraffin wax removal. Certain acid treatments require that wellbore be flushed before injection of acid downhole. This is to reduce the temperature of wellbore system. This problem becomes more severe in deeper wells. Certain acids have very high rates of corrosion at high temperatures. Injection model presented will allow the planning of such acid treatments. It will allow users to calculate the time needed for the cooling of wellbore, flow rate required to achieve the cooling, net amount of fluid required and temperature at which the injection should be done. In case of paraffin wax removal, it was shown that effectiveness of the hot fluid treatment is dependent on injection temperature. Additionally, injected fluid temperature is higher than the geothermal gradient down till a certain depth. After that point the temperature of injected fluid is much lower than the geothermal gradient. The intersection point of geothermal gradient and injected fluid temperature represents the limit of effectiveness of the injection treatment.

Sixth chapter deals with the transient temperature of static borehole mud column. This problem has been modeled as a radial conduction in a multilayer cylinder. Borehole mud

column has been modeled as multilayer cylinder with mud present in annulus and tubing as the two layers. Radial heat conduction equation was solved with steady state mud temperature calculated using Kabir et al. (1996) model as the initial condition and static formation temperature as the boundary condition at the borehole mud - borehole wall interface. Thermal contact resistance at the interface was modeled by bringing in the concept of effective thermal conductivity.

All the solutions presented in this thesis are either analytical or semianalytical. One of the qualities of analytical solutions apart from being accurate is they take less time for calculation. All of the results presented here were calculated using MS Excel. All solutions are very simple and can be applied easily.

REFERENCES

Alves, I., Alhanati, F., and Shoham, O. 1992. A Unified Model for Predicting Flowing Temperature Distribution in Wellbores and Pipelines. *SPE Production Engineering* **7** (4): 363-367. SPE-20632-PA. http://dx.doi.org/10.2118/20632-PA

Arnold, F.C. 1989. Temperature Profiles During Heated Liquid Injection. *International Communications in Heat and Mass Transfer* **16** (6): 763-772. http://dx.doi.org/10.1016/0735-1933(89)90002-X

Bahonar, M., Azaiez, J., and Chen, Z.J. 2011. Transient Nonisothermal Fully Coupled Wellbore/Reservoir Model for Gas-Well Testing, Part 2: Applications. *Journal of Canadian Petroleum Technology* **50** (9-10): 51-70. SPE-149618-PA. http://dx.doi.org/10.2118/149618-PA

Bulavin, P. and Kashcheev, V. 1965. Solution of the Non-Homogeneous Heat Conduction Equation for Multilayered Bodies(Inhomogeneous Thermal Conductivity Equation for Multilayer Plates, Cylinders and Spheres). *International Chemical Engineering* **5**: 112-115.

Chen, N.H. 1979. An Explicit Equation for Friction Factor in Pipe. *Industrial & Engineering Chemistry Fundamentals* **18** (3): 296-297. http://dx.doi.org/10.1021/i160071a019

Coulter, D. and Bardon, M. 1979. Revised Equation Improves Flowing Gas Temperature Prediction. *Oil & Gas J* **77** (9): 107-115.

De Monte, F. 2003. Unsteady Heat Conduction in Two-Dimensional Two Slab-Shaped Regions. Exact Closed-Form Solution and Results. *International Journal of Heat and Mass Transfer* **46** (8): 1455-1469. http://dx.doi.org/10.1016/S0017-9310(02)00417-9

Dranchuk, P.M., Purvis, R.A., and Robinson, D.B. 1973. Computer Calculation of Natural Gas Compressibility Factors Using the Standing and Katz Correlation. Paper PETSOC-73-112 presented at the Annual Technical Meeting, Edmonton, Canada, http://dx.doi.org/10.2118/73-112

Dropkin, D. and Somerscales, E. 1965. Heat Transfer by Natural Convection in Liquids Confined by Two Parallel Plates Which Are Inclined at Various Angles with Respect to the Horizontal. *Journal of Heat Transfer* **87** (1): 77-82. http://dx.doi.org/10.1115/1.3689057

Eickmeier, J., Ersoy, D., and Ramey, H. 1970. Wellbore Temperatures and Heat Losses During Production or Injection Operations. *Journal of Canadian Petroleum Technology* **9** (02): 115-121. PETSOC-70-02-08. http://dx.doi.org/10.2118/70-02-08

Guo, B., Duan, S., and Ghalambor, A. 2004. A Simple Model for Predicting Heat Loss and Temperature Profiles in Thermal Injection Lines and Wellbores with Insulations. Paper SPE-86983-MS presented at the SPE International Thermal Operations and Heavy Oil Symposium and Western Regional Meeting, Bakersfield, California, 16-18 March. http://dx.doi.org/10.2118/86983-MS

Guo, B., Duan, S., and Ghalambor, A. 2006. A Simple Model for Predicting Heat Loss and Temperature Profiles in Insulated Pipelines. *SPE Production & Operations* **21** (1): 107-113. SPE-86983-PA. http://dx.doi.org/10.2118/86983-PA

Hagoort, J. 2004. Ramey's Wellbore Heat Transmission Revisited. *SPE Journal* **9** (4): 465-474. SPE-87305-PA. http://dx.doi.org/10.2118/87305-PA

Hagoort, J. 2005. Prediction of Wellbore Temperatures in Gas Production Wells. *Journal of Petroleum Science and Engineering* **49** (1): 22-36. http://dx.doi.org/10.1016/j.petrol.2005.07.003

Hasan, A.R. and Kabir, C.S. 1991. Heat Transfer During Two-Phase Flow in Wellbores; Part I--Formation Temperature. Paper SPE-22866-MS presented at the SPE Annual Technical Conference and Exhibition, Dallas, Texas, 6-9 October. http://dx.doi.org/10.2118/22866-MS

Hasan, A.R. and Kabir, C.S. 1994. Aspects of Wellbore Heat Transfer During Two-Phase Flow (Includes Associated Papers 30226 and 30970). *SPE Production & Facilities* **9** (3): 211-216. SPE-22948-PA. http://dx.doi.org/10.2118/22948-PA

Hasan, A.R., Kabir, C.S., and Lin, D. 2005. Analytic Wellbore-Temperature Model for Transient Gas-Well Testing. *SPE Reservoir Evaluation & Engineering* **8** (3): 240-247. SPE-84288-PA. http://dx.doi.org/10.2118/84288-PA

Hasan, A.R., Kabir, C.S., and Wang, X. 2009. A Robust Steady-State Model for Flowing-Fluid Temperature in Complex Wells. *SPE Production & Operations* **24** (2): 269-276. SPE-109765-PA. http://dx.doi.org/10.2118/109765-PA

Huenges, E. and Ledru, P. 2010. Geothermal Energy Systems: Exploration, Development, and Utilization, first edition. Weinheim: Wiley-VCH.

Kabir, C.S., Hasan, A.R., Kouba, G.E. et al. 1996. Determining Circulating Fluid Temperature in Drilling Workover and Well Control Operations. *SPE Drilling & Completion* **11** (02): 74-79. SPE-24581-PA. http://dx.doi.org/10.2118/24581-PA

Kestin, J., Khalifa, H.E., Abe, Y. et al. 1978. Effect of Pressure on the Viscosity of Aqueous Sodium Chloride Solutions in the Temperature Range 20-150 °C. *Journal of Chemical and Engineering Data* **23** (4): 328-336. http://dx.doi.org/10.1021/je60079a011

Kirkpatrick, C. 1959. Advances in Gas-Lift Technology. Paper API-59-024 presented at the Drilling and Production Practice, New York, New York, 1 January.

Maury, V. and Guenot, A. 1995. Practical Advantages of Mud Cooling Systems for Drilling. *SPE Drilling & Completion* **10** (01): 42-48. SPE-25732-PA. http://dx.doi.org/10.2118/25732-PA

Moss, J. and White, P. 1959. How to Calculate Temperature Profiles in a Water Injection Well. *Oil and Gas J* **57** (11): 174.

Ramey , H.J. 1962. Wellbore Heat Transmission. *Journal of Petroleum Technology* **14** (4): 427-435. SPE-96-PA. http://dx.doi.org/10.2118/96-PA

Sagar, R., Doty, D.R., and Schmidt, Z. 1991. Predicting Temperature Profiles in a Flowing Well. *SPE Production Engineering* **6** (4): 441-448. SPE-19702-PA. http://dx.doi.org/10.2118/19702-PA

Satter, A. 1965. Heat Losses During Flow of Steam Down a Wellbore. *Journal of Petroleum Technology* **17** (7): 845-851. SPE-1071-PA. http://dx.doi.org/10.2118/1071-PA

Shiu, K. and Beggs, H. 1980. Predicting Temperatures in Flowing Oil Wells. *Journal of Energy Resources Technology* **102** (1): 2-11. http://dx.doi.org/10.1115/1.3227845

Singh, S. and Jain, P.K. 2008. Analytical Solution to Transient Heat Conduction in Polar Coordinates with Multiple Layers in Radial Direction. *International Journal of Thermal Sciences* **47** (3): 261-273. http://dx.doi.org/10.1016/j.ijthermalsci.2007.01.031

Spindler, R. 2011. Analytical Models for Wellbore-Temperature Distribution. *SPE Journal* **16** (1): 125-133. SPE-140135-PA. http://dx.doi.org/10.2118/140135-PA

Squier, D., Smith, D., and Dougherty, E. 1962. Calculated Temperature Behavior of Hot-Water Injection Wells. *Journal of Petroleum Technology* **14** (04): 436-440. SPE-95-PA. http://dx.doi.org/10.2118/95-PA

Straub, T., Autry, S., and King, G. 1989. An Investigation into Practical Removal of Downhole Paraffin by Thermal Methods and Chemical Solvents. Paper SPE-18889-MS presented at the SPE Production Operations Symposium, Oklahoma City, Oklahoma, 13-14 March. http://dx.doi.org/10.2118/18889-MS

Willhite, G.P. 1967. Over-All Heat Transfer Coefficients in Steam and Hot Water Injection Wells. *Journal of Petroleum Technology* **19** (05): 607-615. SPE-1449-PA. http://dx.doi.org/10.2118/1449-PA

APPENDIX

Single Rate Production

Following is the attempt to solve the temperature distribution equation Eq. A-8 of Hasan et al. (2005) using Laplace transform. The beauty of this method is that Laplace transform enables us to find the solution of equation using boundary condition and initial condition simultaneously.

$$(1 + C_T)\frac{\partial T_f}{\partial t} - \frac{w}{m}\frac{\partial T_f}{\partial z} = \frac{w}{m}L_R\left[T_{ei}(z) - T_f\right] + \frac{w}{m}\left(\phi - \frac{gsin\alpha}{c_p J g_c}\right) \quad \text{(A-1)}$$

Subject to initial and boundary conditions:

$$T_f(L, t) = T_{eibh} \quad \text{(A-2)}$$

$$T_f(z, 0) = T_{eibh} - (L - z)g_G sin\alpha \quad \text{(A-3)}$$

Application of Laplace transform on both sides of Eqs. A-1, A-2 and A-3 yields:

$$(1 + C_T)sU - (1 + C_T)u(z, 0) - \frac{w}{m}U_z \quad \text{(A-4)}$$

$$= \frac{wL_R}{ms}[T_{eibh} - (L - z)g_G sin\alpha - sU] + \frac{w}{ms}\left(\phi - \frac{gsin\alpha}{c_p J g_c}\right)$$

$$u(z, 0) = T_{eibh} - (L - z)g_G sin\alpha \quad \text{(A-5)}$$

$$u(L, t) = T_{eibh}/s \quad \text{(A-6)}$$

Substitute Eq. A-5 in to Eq. A-4 yields:

$$U_z - \left(\frac{(1+C_T)s + \frac{w}{m}L_R}{\frac{w}{m}}\right)U \tag{A-7}$$

$$= -\left(\frac{(1+C_T)s + \frac{w}{m}L_R}{\frac{sw}{m}}\right)(T_{eibh} - (L-z)g_G sin\alpha)$$

$$-\frac{1}{s}\left(\phi - \frac{gsin\alpha}{c_p J g_c}\right)$$

Eq. A-7 is first order ordinary differential equation.

Integration factor is given by:

$$\mu = exp\left(-\int \frac{(1+C_T)s + \frac{w}{m}L_R}{\frac{w}{m}}dz\right) = e^{-\left(\frac{(1+C_T)s+\frac{w}{m}L_R}{\frac{w}{m}}\right)z} \tag{A-8}$$

Multiply Eq. A-7 by integration factor given in Eq. A-8.

$$e^{-\left(\frac{(1+C_T)s+\frac{w}{m}L_R}{w/m}\right)z}U_z - e^{-\left(\frac{(1+C_T)s+\frac{w}{m}L_R}{\frac{w}{m}}\right)z}\left(\frac{(1+C_T)s + \frac{w}{m}L_R}{\frac{w}{m}}\right)U \tag{A-9}$$

$$= -e^{-\left(\frac{(1+C_T)s+\frac{w}{m}L_R}{\frac{w}{m}}\right)z}\left(\frac{(1+C_T)s + \frac{w}{m}L_R}{\frac{sw}{m}}\right)(T_{eibh}$$

$$-(L-z)g_G sin\alpha) - e^{-\left(\frac{(1+C_T)s+\frac{w}{m}L_R}{\frac{w}{m}}\right)z}\left(\frac{1}{s}\right)\left(\phi - \frac{gsin\alpha}{c_p J g_c}\right)$$

Rearranging Eq. A-9 yields:

$$\frac{d}{dz}\left[e^{-\left(\frac{(1+C_T)s+\frac{w}{m}L_R}{\frac{w}{m}}\right)z}U\right] \tag{A-10}$$

$$= -e^{-\left(\frac{(1+C_T)s+\frac{w}{m}L_R}{\frac{w}{m}}\right)z}\left(\frac{(1+C_T)s+\frac{w}{m}L_R}{\frac{sw}{m}}\right)(T_{eibh}$$

$$-(L-z)g_G sin\alpha) - e^{-\left(\frac{(1+C_T)s+\frac{w}{m}L_R}{\frac{w}{m}}\right)z}\left(\frac{1}{s}\right)\left(\phi - \frac{gsin\alpha}{c_p J g_c}\right)$$

Integration of Eq. A-10 gives:

$$U = \frac{\frac{w}{m}\psi}{s((1+C_T)s+\frac{w}{m}L_R)} + \frac{1}{s}[T_{eibh} - (L-z)g_G sin\alpha] \tag{A-11}$$

$$+ c_1 e^{\left(\frac{(1+C_T)s+\frac{w}{m}L_R}{\frac{w}{m}}\right)z}$$

where c_1 is integration constant and

$$\psi = g_G \sin\alpha + \phi - \frac{g\sin\alpha}{c_p J g_c} \tag{A-12}$$

Application of boundary condition Eq. A-6 to Eq. A-11 lets us find integration constant c_1 as:

$$c_1 = -\left[\frac{\frac{w}{m}\psi}{s\left((1+C_T)s+vL_R\right)}\right]e^{-\left(\frac{(1+C_T)s+\frac{w}{m}L_R}{\frac{w}{m}}\right)L} \tag{A-13}$$

Substitute c_1 from Eq. A-13 into Eq. A-11 gives:

$$U = \frac{\frac{w}{m}\psi}{s((1+C_T)s+\frac{w}{m}L_R)} + \frac{1}{s}[T_{eibh} - (L-z)g_G sin\alpha] \tag{A-14}$$

$$+\left(-\frac{\frac{w}{m}\psi}{s\left((1+C_T)s+\frac{w}{m}L_R\right)}\right)e^{-\left(\frac{(1+C_T)s+\frac{w}{m}L_R}{\frac{w}{m}}\right)(L-z)}$$

Application of Laplace Inverse transform to Eq. A-14 gives:

$$T_f = T_{ei}(z) + \frac{\psi}{L_R}\left[1 - e^{-\frac{wL_R}{m(1+C_T)}t}\right. \tag{A-15}$$

$$\left. -\left(e^{-(L-z)L_R} - e^{-\frac{wL_R}{m(1+C_T)}t}\right)H\langle t - \frac{(1+C_T)(L-z)}{\frac{w}{m}}\rangle\right]$$

where H is Heaviside function given by:

$$H\left(t - \frac{(1+C_T)(L-z)}{\frac{w}{m}}\right) = \begin{cases} 0, & t - \frac{(1+C_T)(L-z)}{\frac{w}{m}} \leq 0 \\ 1, & t - \frac{(1+C_T)(L-z)}{\frac{w}{m}} > 0 \end{cases} \tag{A-16}$$

Since Heaviside is a step function it causes abrupt discontinuity in the temperature profile. This has to be replaced with Logistic as follows. Logistic function equation is given by:

$$y = D + \frac{(A-D)}{1+\left(\frac{x}{C}\right)^{\hat{B}}} \tag{A-17}$$

where

A = minimum asymptote

$\hat{B}$ = slope factor

C = inflection point

D = maximum asymptote

For our case

$x = z$ (A-18)

$y = \hat{m}$ (A-19)

$A = 0$ (A-20)

$C = z'_{prod}$ (A-21)

$D = 1$ (A-22)

where z'_{prod} is defined as the depth where condition given by the following equation is true:

$$z'_{prod} = L - \frac{vt}{1 + C_T} \quad \text{(A-23)}$$

Substitute the values of x, y, A, C and D into Eq. A-17

$$\hat{m} = 1 - \frac{1}{1 + \left(\frac{z}{z'_{prod}}\right)^{\hat{B}}} \quad \text{(A-24)}$$

$\hat{B}$ can be calculated as follows:

Define

$$\hat{m} = 0.99 \; at \; z = L \quad \text{(A-25)}$$

Substitute Eq. A-25 into Eq. A-24

$$0.99 = 1 - \frac{1}{1 + \left(\frac{L}{z'_{prod}}\right)^{\hat{B}}} \quad \text{(A-26)}$$

After rearranging and taking natural log of both sides of Eq. A-26 we get:

$$\hat{B} = \frac{4.59}{ln\left(\frac{L}{z'_{prod}}\right)} \tag{A-27}$$

Heaviside function in Eq. A-15 is replaced with Logistic function and the final transient temperature equation is given by:

$$T_f = T_{ei}(z) + \frac{\psi}{L_R}\left[1 - e^{-\frac{wL_R}{m(1+C_T)}t} - \left(e^{-(L-z)L_R} - e^{-\frac{wL_R}{m(1+C_T)}t}\right)\hat{m}\right] \tag{A-28}$$

Where

$$\hat{m} = \begin{cases} 1 - \dfrac{1}{1 + \left(\dfrac{z}{z'_{prod}}\right)^{\hat{B}}}, & L > z'_{prod} > 0 \\ 1, & z'_{prod} = 0 \; or \; z'_{prod} \geq L \end{cases} \tag{A-29}$$

$\hat{B}$ and z'_{prod} are given by Eqs. A-27 and A-23.

Equations for various parameters required to calculate temperature using Eq. A-28 are being reproduced here from Hasan et al. (2005) and Hasan and Kabir (1994).

$$L_R = \frac{2\pi}{c_p w}\left[\frac{r_{to}U_{to}k_e}{k_e + r_{to}U_{to}T_D}\right] \tag{A-30}$$

$$T_D = ln[e^{-0.2t_D} + (1.5 - 0.3719e^{-t_D})]\sqrt{t_D} \tag{A-31}$$

$$t_D = \alpha_e t / r_w^2 \tag{A-32}$$

$$\phi = C_J \frac{dp}{dz} - \frac{vdv}{g_c J c_p} \tag{A-33}$$

Single Rate Injection

For the case of injection following temperature distribution is solved:

$$(1+C_T)\frac{\partial T_f}{\partial t}+\frac{w}{m}\frac{\partial T_f}{\partial z}=\frac{w}{m}L_R\left[T_{ei}(z)-T_f\right]-\frac{w}{m}\left(\phi-\frac{gsin\alpha}{c_pJg_c}\right) \tag{A-34}$$

Subject to initial and boundary conditions:

$$T_f(0,t)=T_{fwh} \tag{A-35}$$

$$T_f(z,0)=T_{sur}+zg_G\sin\alpha \tag{A-36}$$

Application of Laplace transform on both sides of Eqs. A-34, A-35 and A-36 yields:

$$(1+C_T)sU+(1+C_T)u(z,0)-\frac{w}{m}U_z \tag{A-37}$$

$$=\frac{wL_R}{ms}[T_{sur}+zg_Gsin\alpha-sU]-\frac{w}{ms}\left(\phi-\frac{gsin\alpha}{c_pJg_c}\right)$$

$$u(z,0)=T_{sur}+zg_G\sin\alpha \tag{A-38}$$

$$u(0,t)=T_{fwh}/s \tag{A-39}$$

Substitute Eq. A-38 in to Eq. A-37 yields:

$$U_z+\left(\frac{(1+C_T)s+\frac{w}{m}L_R}{\frac{w}{m}}\right)U \tag{A-40}$$

$$=\left(\frac{(1+C_T)s+\frac{w}{m}L_R}{\frac{sw}{m}}\right)(T_{sur}+zg_G\sin\alpha)-\frac{1}{s}\left(\phi-\frac{g\sin\alpha}{c_pJg_c}\right)$$

Eq. A-40 is first order ordinary differential equation.

Integration factor is given by:

$$\mu = exp\left(\int \frac{(1+C_T)s + \frac{w}{m}L_R}{\frac{w}{m}}\,dz\right) = e^{\left(\frac{(1+C_T)s+\frac{w}{m}L_R}{\frac{w}{m}}\right)z} \tag{A-41}$$

Multiply Eq. A-40 by integration factor given in Eq.A-41.

$$e^{\left(\frac{(1+C_T)s+\frac{w}{m}L_R}{w/m}\right)z}U_z + e^{\left(\frac{(1+C_T)s+\frac{w}{m}L_R}{\frac{w}{m}}\right)z}\left(\frac{(1+C_T)s+\frac{w}{m}L_R}{\frac{w}{m}}\right)U \tag{A-42}$$

$$= e^{\left(\frac{(1+C_T)s+\frac{w}{m}L_R}{\frac{w}{m}}\right)z}\left(\frac{(1+C_T)s+\frac{w}{m}L_R}{\frac{sw}{m}}\right)(T_{sur} + zg_G sin\alpha)$$

$$- e^{\left(\frac{(1+C_T)s+\frac{w}{m}L_R}{\frac{w}{m}}\right)z}\left(\frac{1}{s}\right)\left(\phi - \frac{gsin\alpha}{c_p J g_c}\right)$$

Rearranging Eq. A-42 yields

$$\frac{d}{dz}\left[e^{\left(\frac{(1+C_T)s+\frac{w}{m}L_R}{\frac{w}{m}}\right)z}U\right] \tag{A-43}$$

$$= e^{\left(\frac{(1+C_T)s+\frac{w}{m}L_R}{\frac{w}{m}}\right)z}\left(\frac{(1+C_T)s+\frac{w}{m}L_R}{\frac{sw}{m}}\right)(T_{sur} + zg_G \sin\alpha)$$

$$- e^{\left(\frac{(1+C_T)s+\frac{w}{m}L_R}{\frac{w}{m}}\right)z}\left(\frac{1}{s}\right)\left(\phi - \frac{g\sin\alpha}{c_p J g_c}\right)$$

Integration of Eq. A-43 gives:

$$U = -\frac{\frac{w}{m}\psi}{s((1+C_T)s+\frac{w}{m}L_R)} + \frac{1}{s}[T_{sur} + zg_G\sin\alpha] + c_1 e^{-\left(\frac{(1+C_T)s+\frac{w}{m}L_R}{\frac{w}{m}}\right)z} \quad \text{(A-44)}$$

where c_1 is integration constant and

$$\psi = g_G\sin\alpha + \phi - \frac{g\sin\alpha}{c_p J g_c} \quad \text{(A-45)}$$

Application of boundary condition Eq.A-39 to Eq. A-44 lets us find integration constant c_1 as:

$$c_1 = \frac{\frac{w}{m}\psi}{s\left((1+C_T)s+vL_R\right)} + \frac{T_{fwh}-T_{sur}}{s} \quad \text{(A-46)}$$

Substitute c_1 from Eq. A-46 into Eq. A-44 gives:

$$U = -\frac{\frac{w}{m}\psi}{s((1+C_T)s+\frac{w}{m}L_R)} + \frac{1}{s}[T_{sur} + zg_G\sin\alpha] \quad \text{(A-47)}$$

$$+\left(\frac{T_{fwh}-T_{sur}}{s} + \frac{\frac{w}{m}\psi}{s\left((1+C_T)s+\frac{w}{m}L_R\right)}\right)e^{-\left(\frac{(1+C_T)s+\frac{w}{m}L_R}{\frac{w}{m}}\right)z}$$

Application of Laplace Inverse transform to Eq. A-47 gives:

$$T_f = T_{sur} + zg_G\sin\alpha \quad \text{(A-48)}$$

$$-\frac{\psi}{L_R}\left[1 - e^{-\frac{wL_R}{m(1+C_T)}t} + e^{-\frac{wL_R}{m(1+C_T)}t} H\langle t - \frac{(1+C_T)z}{\frac{w}{m}}\rangle\right]$$

$$+\left(T_{fwh} - T_{sur} + \frac{\psi}{L_R}\right)e^{-zL_R} H\langle t - \frac{(1+C_T)z}{\frac{w}{m}}\rangle$$

where H is Heaviside function given by:

$$H\left(t-\frac{(1+C_T)z}{\frac{w}{m}}\right)=\begin{cases}0, & t-\frac{(1+C_T)z}{\frac{w}{m}}\leq 0\\ 1, & t-\frac{(1+C_T)z}{\frac{w}{m}}>0\end{cases} \quad \text{(A-49)}$$

Since Heaviside is a step function it causes abrupt discontinuity in the temperature profile. This has to be replaced with Logistic function as follows. Logistic function equation is given by:

$$y=D+\frac{(A-D)}{1+\left(\frac{x}{C}\right)^{\breve{B}}} \quad \text{(A-50)}$$

where

A = maximum asymptote

$\breve{B}$ = slope factor

C = inflection point

D = minimum asymptote

For our case

$x = z$ (A-51)

$y=\breve{m}$ (A-52)

$A = 1$ (A-53)

$C=z'_{inj}$ (A-54)

$D = 0$ (A-55)

where z'_{inj} is defined as the depth where the condition given by the following equation is true:

$$z = \frac{vt}{1 + C_T} \tag{A-56}$$

Substitute the values of x, y, A, C and D into Eq. A-50

$$\breve{m} = \frac{1}{1 + \left(\frac{z}{z'_{inj}}\right)^{\breve{B}}} \tag{A-57}$$

$\breve{B}$ can be calculated as follows:

Define

$$\breve{m} = 0.01 \; at \; z = L \tag{A-58}$$

Substitute Eq. A-58 into Eq. A-57

$$0.01 = \frac{1}{1 + \left(\frac{L}{z'_{inj}}\right)^{\breve{B}}} \tag{A-59}$$

After rearranging and taking natural log of both sides of Eq. A-59 we get:

$$\breve{B} = \frac{4.59}{ln\left(\frac{L}{z'_{inj}}\right)} \tag{A-60}$$

Heaviside function in Eq. A-48 is replaced with Logistic function and the final transient temperature equation is given by:

$$T_f = T_{sur} + z g_G sin\alpha \; - \frac{\psi}{L_R}\left[1 - e^{-\frac{wL_R}{m(1+C_T)}t} + e^{-\frac{wL_R}{m(1+C_T)}t}\breve{m}\right] \tag{A-61}$$

$$+ \left(T_{fwh} - T_{sur} + \frac{\psi}{L_R}\right) e^{-zL_R}\breve{m}$$

where

$$\breve{m} = \begin{cases} 1 - \dfrac{1}{1 + \left(\dfrac{z}{z'_{inj}}\right)^{\breve{B}}} , & 0 < z'_{inj} < L \\ 1 , & z'_{inj} = 0 \; or \; z'_{inj} \geq L \end{cases} \tag{A-62}$$

B and z' are given by Eqs. A-60 and A-56 respectively.

Arnold (1989) found that, at a certain depth, fluid temperature crosses the formation temperature and this is the depth to which heat treatment is effective. Similarly, our proposed model predicts such depth which can be obtained by substituting formation temperature for fluid temperature for a value of Heaviside function of 1 in Eq. A-48 as follows:

$$T_{ei} = T_{ei} - \frac{\psi}{L_R}\left[1 - e^{-\frac{wL_R}{m(1+C_T)}t} + e^{-\frac{wL_R}{m(1+C_T)}t} \cdot 1\right] + \left(T_{fwh} - T_{sur} + \frac{\psi}{L_R}\right) e^{-zL_R} \cdot 1 \tag{A-63}$$

Rearrangement of above equation leads to:

$$z_{effective} = \frac{1}{L_R} ln\left[\left(\frac{\psi}{L_R}\right)^{-1}\left(\frac{\psi}{L_R} + T_{fwh} - T_{sur}\right)\right] \tag{A-64}$$

Transient Rate Production

For transient rate case, the governing equation would remain the same however different boundary condition will be used.

$$(1+C_T)\frac{\partial T_f}{\partial t}-\frac{w}{m}\frac{\partial T_f}{\partial z}=\frac{w'}{m'}L'_R\left[T_{ei}(z)-T_f\right]+\frac{w'}{m'}\left(\phi'-\frac{gsin\alpha}{c_pJg_c}\right) \quad \text{(A-65)}$$

Subject to initial and boundary conditions:

$$T_f(L,t)=T_{eibh} \quad \text{(A-66)}$$

$$T_f(z,0)=T_f=T_{ei}+\frac{1-e^{-(L-z)L_R}}{L_R}\psi \quad \text{(A-67)}$$

Application of Laplace transform on both sides of Eqs. A-65, A-66 and A-67 yields:

$$(1+C_T)sU-(1+C_T)u(z,0)-\frac{w'}{m'}U_z \quad \text{(A-68)}$$

$$=\frac{w'L'_R}{m's}\left[T_{eibh}-(L-z)g_Gsin\alpha-sU\right]+\frac{w'}{m's}\left(\phi'-\frac{gsin\alpha}{c_pJg_c}\right)$$

$$u(z,0)=\frac{1}{s}\left[T_{eibh}-(L-z)g_Gsin\alpha+\frac{1-e^{-(L-z)L_R}}{L_R}\psi\right] \quad \text{(A-69)}$$

$$u(L,t)=T_{eibh}/s \quad \text{(A-70)}$$

Substitute Eq. A-69 in to Eq. A-68 yields:

$$U_z-\frac{m'}{w'}\left[(1+C_T)s+\frac{w'}{m'}L'_R\right]U \quad \text{(A-71)}$$

$$+\frac{m'}{w'}(1+C_T)\left[T_{eibh}-(L-z)g_G\sin\alpha+\frac{1-e^{-(L-z)L_R}}{L_R}\psi\right]$$

$$+\frac{1}{s}\left[L'_R(T_{eibh}-(L-z)g_G\sin\alpha)+\phi'-\frac{g\sin\alpha}{c_pJg_c}\right]=0$$

Eq. A-71 is first order ordinary differential equation.

Integration factor is given by:

$$\mu = exp\left(-\int \frac{m'}{w'}\left[(1+C_T)s + \frac{w'}{m'}L'_R\right]dz\right) = e^{-\frac{m'}{w'}\left[(1+c_T)s+\frac{w'}{m'}L'_R\right]z} \tag{A-72}$$

Multiply Eq. A-71 by integration factor given in Eq.A-72.

$$e^{-\frac{m'}{w'}\left[(1+C_T)s+\frac{w'}{m'}L'_R\right]z}U_z - e^{-\frac{m'}{w'}\left[(1+C_T)s+\frac{w'}{m'}L'_R\right]z}\frac{m'}{w'}\left[(1+C_T)s + \frac{w'}{m'}L'_R\right]U \tag{A-73}$$

$$+\ e^{-\frac{m'}{w'}\left[(1+C_T)s+\frac{w'}{m'}L'_R\right]z}\frac{m'}{w'}(1+C_T)\left[T_{eibh} - (L-z)g_G sin\alpha\right.$$

$$\left.+\ \frac{1-e^{-(L-z)L_R}}{L_R}\psi\right]$$

$$+\frac{e^{-\frac{m'}{w'}\left[(1+C_T)s+\frac{w'}{m'}L'_R\right]z}}{s}\left[L'_R(T_{eibh} - (L-z)g_G sin\alpha) + \phi'\right.$$

$$\left.-\frac{gsin\alpha}{c_p J g_c}\right] = 0$$

Rearranging Eq. A-73 yields

$$\frac{d}{dz}\left[e^{-\frac{m'}{w'}\left[(1+C_T)s+\frac{w'}{m'}L'_R\right]z}U\right] \tag{A-74}$$

$$= -e^{-\frac{m'}{w'}\left[(1+C_T)s+\frac{w'}{m'}L'_R\right]z}\frac{m'}{w'}(1+C_T)\left[T_{eibh}-(L-z)g_G sin\alpha\right.$$

$$\left.+\frac{1-e^{-(L-z)L_R}}{L_R}\psi\right]$$

$$-\frac{e^{-\frac{m'}{w'}\left[(1+C_T)s+\frac{w'}{m'}L'_R\right]z}}{s}\left[L'_R(T_{eibh}-(L-z)g_G sin\alpha)+\phi'\right.$$

$$\left.-\frac{gsin\alpha}{c_p J g_c}\right]$$

For maintaining the readability of derivation lets define:

$$K = -\frac{m'}{w'}\left[(1+C_T)s+\frac{w'}{m'}L'_R\right] \tag{A-75}$$

Integration of Eq. A-74 gives:

$$U = \left[-\frac{m'}{w'}(1+C_T)T_{eibh}\cdot\frac{1}{K}+\frac{m'}{w'}(1+C_T)g_G L\sin\alpha\cdot\frac{1}{K}\right. \tag{A-76}$$

$$-\left(\frac{m'(1+C_T)g_G\sin\alpha}{w'}+\frac{g_G\sin\alpha L'_R}{s}\right)\cdot\frac{1}{K}\cdot\left(z-\frac{1}{K}\right)$$

$$-\frac{m'(1+C_T)}{w'}\cdot\frac{\psi}{L_R}\cdot\frac{1}{K}+\frac{m'}{w'}(1+C_T)\frac{\psi}{L_R}\cdot\frac{e^{-LL_R+zL_R}}{K+L_R}$$

$$\left.-\frac{1}{sK}\left[L'_R(T_{eibh}-g_G L\sin\alpha)+\phi'-\frac{g\sin\alpha}{c_p J g_c}\right]\right]+c_1 e^{-Kz}$$

where c_1 is integration constant and

$$\psi = g_G \sin\alpha + \phi - \frac{g\sin\alpha}{c_f J g_c} \tag{A-77}$$

Application of boundary condition Eq. A-70 to Eq. A-76 lets us find integration constant c_1 as:

$$\begin{aligned} c_1 = -\Bigg[& -\frac{T_{eibh}}{s} - \frac{m'}{w'}(1+C_T)T_{eibh} \cdot \frac{1}{K} + \frac{m'}{w'}(1+C_T) g_G L \sin\alpha \cdot \frac{1}{K} \\ & - \left(\frac{m'(1+C_T) g_G \sin\alpha}{w'} + \frac{g_G \sin\alpha L'_R}{s} \right) \cdot \frac{1}{K} \cdot \left(L - \frac{1}{K} \right) \\ & - \frac{m'(1+C_T)}{w'} \cdot \frac{\psi}{L_R} \cdot \frac{1}{K} + \frac{m'}{w'}(1+C_T) \frac{\psi}{L_R} \cdot \frac{e^{-LL_R + LL_R}}{K + L_R} \\ & - \frac{1}{sK} \left[L'_R (T_{eibh} - g_G L \sin\alpha) + \phi' - \frac{g\sin\alpha}{c_p J g_c} \right] \Bigg] e^{KL} \end{aligned} \tag{A-78}$$

Substitute c_1 from Eq. A-78 into Eq. A-76 gives:

$$\begin{aligned} U = \frac{m'}{w'}(1+C_T) \Bigg[& -\frac{T_{eibh}}{K} + \frac{g_G L \sin\alpha}{K} - \frac{g_G \sin\alpha}{K} \left(z - \frac{1}{K} \right) - \frac{\psi}{K \cdot L_R} + \frac{\psi}{L_R} \\ & \cdot \frac{e^{-LL_R + zL_R}}{K + L_R} \Bigg] \\ & - \frac{1}{sK} \Bigg[g_G \sin\alpha L'_R \left(z - \frac{1}{K} \right) + L'_R T_{eibh} - LL'_R g_G \sin\alpha \\ & + \left(\phi - \frac{g\sin\alpha}{c_p J g_c} \right) \Bigg] + [\frac{T_{eibh}}{s} \\ & - \frac{m'}{w'}(1+C_T) \left[-\frac{T_{eibh}}{K} + \frac{g_G \sin\alpha}{K^2} - \frac{\psi}{K \cdot L_R} + \frac{\psi}{L_R(K + L_R)} \right] \\ & + \frac{1}{sK} \left[-\frac{g_G \sin\alpha L'_R}{K} + L'_R T_{eibh} + \left(\phi - \frac{g\sin\alpha}{c_p J g_c} \right) \right] e^{K(L-z)} \end{aligned} \tag{A-79}$$

Application of Laplace Inverse transform to Eq. A-79 gives:

$$T_f = T_{ei}(z) + \frac{\psi'}{L_R'}\left(1 - e^{A't}\right) + \frac{\psi}{L_R} e^{A't}\left(1 - e^{-At-(L-z)L_R}\right) \tag{A-80}$$

where

$$A' = -\frac{w'}{m'} \cdot \frac{L_R'}{1 + C_T} \tag{A-81}$$

$$A = -\frac{w'}{m'} \cdot \frac{L_R}{1 + C_T} \tag{A-82}$$

$$\psi' = g_G \sin\alpha + \phi' - \frac{g \sin\alpha}{c_p J g_c} \tag{A-83}$$

when

$$H\left(t - \frac{m'}{w'}(1 + C_T)(L - z)\right) = 0 \tag{A-84}$$

and

$$T_f = T_{ei}(z) + \frac{\psi'}{L_R'}\left(1 - e^{-L_R'(L-z)}\right) \tag{A-85}$$

when

$$H\left(t - \frac{m'}{w'}(1 + C_T)(L - z)\right) = 1 \tag{A-86}$$

where values of Heaviside functions in Eqs. A-84 and A-86 are determined by Eq. A-87.

$$H\left(t - \frac{m'}{w'}(1 + c_T)(L - z)\right) = \begin{cases} 0 & t - \frac{m'}{w'}(1 + c_T)(L - z) \leq 0 \\ 1 & t - \frac{m'}{w'}(1 + c_T)(L - z) > 0 \end{cases} \tag{A-87}$$

Transient Temperature of Mud after Cessation of Circulation

Heat transfer in static borehole mud has been modeled as conduction through a concentric cylinder. Fig. 19 shows the cross section of a multilayer concentric cylinder.

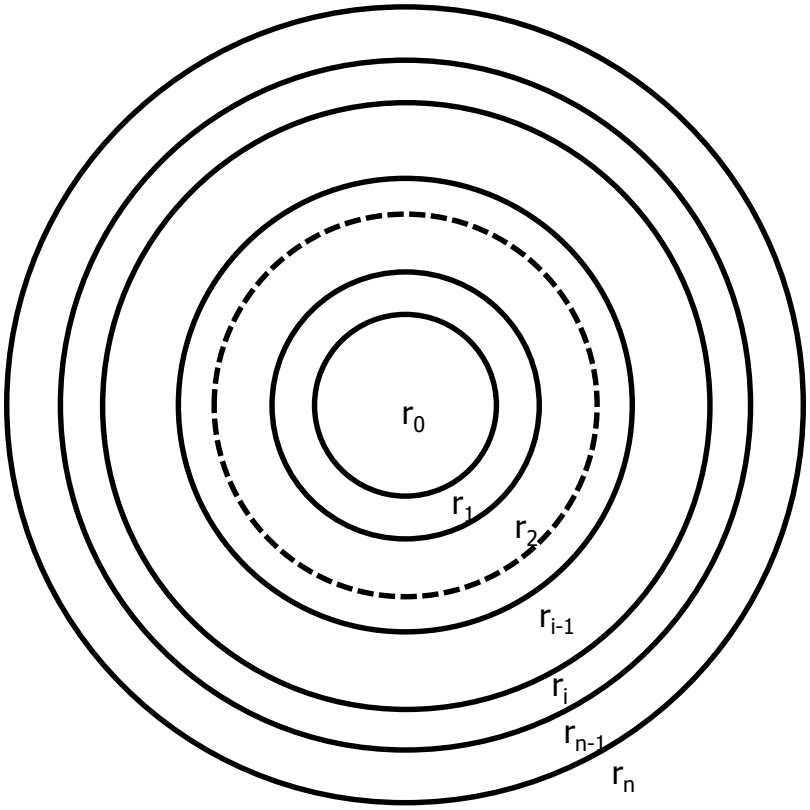

Fig. 19-Cross section of a multilayer concentric cylinder

Heat conduction equation in radial coordinates for such multilayer concentric cylinder can be written as follows:

$$\frac{\partial^2 T_i}{\partial r^2} + \frac{1}{r}\frac{\partial T_i}{\partial r} - \frac{1}{\alpha_i}\frac{\partial T_i}{\partial t} = 0 \qquad \text{(A-88)}$$

Initial condition:

$$T_i(r,0) = X_i = constant \tag{A-89}$$

Boundary conditions:

For i = 1

$$T_1(0,t) = finite \tag{A-90}$$

Outer surface of nth annulus:

$$T_n(r = r_n, t\ ) = T_{ei} \tag{A-91}$$

Inner interface of ith layer:

$$T_i(r_{i-1}\ , t) = T_{i-1}\ (r_{i-1}, t) \tag{A-92}$$

$$\frac{k_i \partial T_i(r_{i-1}, t)}{\partial r} = \frac{k_{i-1} \partial T_{i-1}(r_i, t)}{\partial r} \tag{A-93}$$

Outer interface of ith layer

$$T_i(r_i\ , t) = T_{i+1}\ (r_i, t) \tag{A-94}$$

$$\frac{k_i \partial T_i(r_i, t)}{\partial r} = \frac{k_{i+1} \partial T_{i+1}(r_i, t)}{\partial r} \tag{A-95}$$

Interface conditions given by Eqs. A-92 to A-95 are necessary for continuous heat flux.(De Monte 2003)

Substitute

$$T_i = \breve{T}_\iota + T_{ss,i} \tag{A-96}$$

into Eqs. A-88 through A-95.

$$\frac{\partial^2 \breve{T}_i}{\partial r^2} + \frac{1}{r}\frac{\partial \breve{T}_i}{\partial r} - \frac{1}{\alpha_i}\frac{\partial \breve{T}_i}{\partial t} + \frac{\partial^2 T_{ss,i}}{\partial r^2} + \frac{1}{r}\frac{\partial T_{ss,i}}{\partial r} = 0 \tag{A-97}$$

Boundary conditions:

$$\check{T}_1(0,t) + T_{ss,1} = finite \tag{A-98}$$

$$\check{T}_n(r = r_n, t) + T_{ss,n}(r = r_n, t) = T_{ei} \tag{A-99}$$

Inner interface of ith layer:

$$T_{ss,i}(r_{i-1}, t) + \check{T}_i(r_{i-1}, t) = T_{ss,i-1}(r_{i-1}, t) + \check{T}_{i-1}(r_{i-1}, t) \tag{A-100}$$

$$\frac{k_i \partial \check{T}_i(r_{i-1}, t)}{\partial r} + \frac{k_i \partial T_{ss,i}(r_{i-1}, t)}{\partial r} = \frac{k_{i-1} \partial \check{T}_{i-1}(r_i, t)}{\partial r} + \frac{k_{i-1} \partial T_{ss,i-1}(r_i, t)}{\partial r} \tag{A-101}$$

Outer interface of ith layer:

$$\check{T}_i(r_i, t) + T_{ss,i}(r_i, t) = \check{T}_{i+1}(r_i, t) + T_{ss,i+1}(r_i, t) \tag{A-102}$$

$$\frac{k_i \partial T_{ss,i}(r_i, t)}{\partial r} + \frac{k_i \partial \check{T}_i(r_i, t)}{\partial r} = \frac{k_{i+1} \partial T_{ss,i+1}(r_i, t)}{\partial r} + \frac{k_{i+1} \partial \check{T}_{i+1}(r_i, t)}{\partial r} \tag{A-103}$$

Now the problem defined by Eq. A-88 has been split into two solvable problems as follows:

Non-homogeneous Steady State Problem

$$\frac{\partial^2 T_{ss,i}}{\partial r^2} + \frac{1}{r}\frac{\partial T_{ss,i}}{\partial r} = 0 \tag{A-104}$$

Boundary conditions:

$$T_{ss,1}(r = r_0) = finite \tag{A-105}$$

$$T_{ss,n}(r = r_n, t) = T_{ei} \tag{A-106}$$

Inner interface of ith layer:

$$T_{ss,i}(r_{i-1}, t) = T_{ss,i-1}(r_{i-1}, t) \tag{A-107}$$

$$\frac{k_i \partial T_{ss,i}(r_{i-1},t)}{\partial r} = \frac{k_{i-1} \partial T_{ss,i-1}(r_i,t)}{\partial r} \quad \text{(A-108)}$$

Outer interface of ith layer

$$T_{ss,i}(r_i\ ,t) = T_{ss,i+1}\ (r_i,t) \quad \text{(A-109)}$$

$$\frac{k_i \partial T_{ss,i}(r_i,t)}{\partial r} = \frac{k_{i+1} \partial T_{ss,i+1}(r_i,t)}{\partial r} \quad \text{(A-110)}$$

General solution of above equation is:

$$T_{ss,i} = A_i lnr + B_i \quad \text{(A-111)}$$

At $r = r_0 = 0 \rightarrow \ln 0 = \infty$ so choose $A_i = 0$

$$T_{ss,i} = B_i \quad \text{(A-112)}$$

$$At\ r = r_n$$

$$T_{ss,n} = T_{ei} \quad \text{(A-113)}$$

so $T_{ss,n} = B_i = T_{ei}$

Thus,

$$T_{ss,i} = T_{ei} \quad \text{(A-114)}$$

It makes sense because temperature of everything inside tubing and annulus will reach earth temperature at some point in time.

Transient Problem

$$\frac{\partial^2 \breve{T}_i}{\partial r^2} + \frac{1}{r}\frac{\partial \breve{T}_i}{\partial r} - \frac{1}{\alpha_i}\frac{\partial \breve{T}_i}{\partial t} = 0 \quad \text{(A-115)}$$

Boundary conditions

$$\breve{T}_1(0,t) = finite \quad \text{(A-116)}$$

$$\check{T}_n(r = r_n, t) = T_{ei} \tag{A-117}$$

Inner interface of ith layer:

$$\check{T}_i(r_{i-1}, t) = \check{T}_{i-1}(r_{i-1}, t) \tag{A-118}$$

$$\frac{k_i \partial \check{T}_i(r_{i-1}, t)}{\partial r} = \frac{k_{i-1} \partial \check{T}_{i-1}(r_i, t)}{\partial r} \tag{A-119}$$

Outer interface of ith layer

$$\check{T}_i(r_i, t) = \check{T}_{i+1}(r_i, t) \tag{A-120}$$

$$\frac{k_i \partial \check{T}_i(r_i, t)}{\partial r} = \frac{k_{i+1} \partial \check{T}_{i+1}(r_i, t)}{\partial r} \tag{A-121}$$

Initial condition:

$$\check{T}_i(r, 0) = X_i = constant \tag{A-122}$$

Apply method of separation of variables.

Let solution be of the form:

$$\check{T}_i = \Gamma_i R_i \tag{A-123}$$

Substitute Eq. A-123 in Eq. A-115 to get:

$$\Gamma_i \frac{\partial^2 R_i}{\partial r^2} + \frac{\Gamma_i}{r} \frac{\partial R_i}{\partial r} - \frac{R_i}{\alpha_i} \frac{\partial \Gamma_i}{\partial t} = 0 \tag{A-124}$$

$$\Gamma_i \frac{\partial^2 R_i}{\partial r^2} + \frac{\Gamma_i}{r} \frac{\partial R_i}{\partial r} = \frac{R_i}{\alpha_i} \frac{\partial \Gamma_i}{\partial t} \tag{A-125}$$

$$\frac{1}{R_i} \frac{\partial^2 R_i}{\partial r^2} + \frac{1}{r R_i} \frac{\partial R_i}{\partial r} = \frac{1}{\alpha_i \Gamma_i} \frac{\partial \Gamma_i}{\partial t} = -\lambda_i^2 \tag{A-126}$$

We get two equations out of Eq. A-126:

$$rR_i'' + R_i' + r\lambda_i^2 R = 0 \tag{A-127}$$

$$\Gamma_i' + \alpha\lambda^2\Gamma_i = 0 \tag{A-128}$$

Solution of Eq. A-128 is:

$$\Gamma_i = c_{1i}e^{-\alpha_i\lambda_{in}^2 t} \tag{A-129}$$

General solution of Eq. A-127 is given by:

$$R_{in}(r) = a_{in}J_0(\lambda_{in}r_i) + b_{in}Y_0(\lambda_{in}r) \tag{A-130}$$

Combining the two solutions given by Eqs. A-129 and A-130 using Eq. A-123:

$$\bar{T}_i = \sum_{n=1}^{\infty} a_n e^{-\alpha_i\lambda_{in}^2 t}R_{in}(\lambda_{in}r) \tag{A-131}$$

Orthogonality condition has to be used in order to evaluate a_n. This proof has been done by Singh and Jain (2008). It is being done here to verify if it is applicable for our case.

Orthogonality Condition Proof

Let R_{ip} and R_{iq} be eigenfunctions satisfying Eq. A-127.

Thus,

$$\frac{1}{r}\frac{d}{dr}\left(r\frac{dR_{ip}}{dr}\right) + \lambda_{ip}^2 R_{ip} = 0 \tag{A-132}$$

$$\frac{1}{r}\frac{d}{dr}\left(r\frac{dR_{iq}}{dr}\right) + \lambda_{iq}^2 R_{iq} = 0 \tag{A-133}$$

Multiply Eq. A-132 by R_{iq} and Eq. A-133 by R_{ip} and subtract:

$$\frac{R_{iq}}{r}\frac{d}{dr}\left(r\frac{dR_{ip}}{dr}\right) - \frac{R_{ip}}{r}\frac{d}{dr}\left(r\frac{dR_{iq}}{dr}\right) + \left(\lambda_{ip}^2 - \lambda_{iq}^2\right)R_{ip}R_{iq} = 0 \tag{A-134}$$

Operate above equation with $\int_{r_{i-1}}^{r_i} rdr$

$$\int_{r_{i-1}}^{r_i} R_{iq}\frac{d}{dr}\left(r\frac{dR_{ip}}{dr}\right)dr - \int_{r_{i-1}}^{r_i} R_{iq}\frac{d}{dr}\left(r\frac{dR_{iq}}{dr}\right)dr + \int_{r_{i-1}}^{r_i} r\left(\lambda_{ip}^2-\lambda_{iq}^2\right)R_{ip}R_{iq}dr = 0 \tag{A-135}$$

Take first integral of above equation and apply integration by parts twice to get:

$$\int_{r_{i-1}}^{r_i} R_{iq}\frac{d}{dr}\left(r\frac{dR_{ip}}{dr}\right)dr = \left[rR_{iq}\frac{dR_{ip}}{dr} - rR_{ip}\frac{dR_{iq}}{dr}\right]_{r=r_{i-1}}^{r=r_i} + \int_{r_{i-1}}^{r_i} R_{iq}\frac{d}{dr}\left(r\frac{dR_{iq}}{dr}\right)dr \tag{A-136}$$

Substitute Eq. A-136 into Eq. A-135.

$$\left[rR_{iq}\frac{dR_{ip}}{dr} - rR_{ip}\frac{dR_{iq}}{dr}\right]_{r=r_{i-1}}^{r=r_i} + \int_{r_{i-1}}^{r_i} r\left(\lambda_{ip}^2-\lambda_{iq}^2\right)R_{ip}R_{iq}dr = 0 \tag{A-137}$$

Multiply above equation by ki and sum over all i.

$$\sum_{i=1}^{n}\left[k_i rR_{iq}\frac{dR_{ip}}{dr} - k_i rR_{ip}\frac{dR_{iq}}{dr}\right]_{r=r_{i-1}}^{r=r_i} + \sum_{i=1}^{n} k_i\int_{r_{i-1}}^{r_i} r\left(\lambda_{ip}^2-\lambda_{iq}^2\right)R_{ip}R_{iq}dr = 0 \tag{A-138}$$

After application of interface conditions

$$\left[k_n rR_{nq}\frac{dR_{np}}{dr} - k_n rR_{np}\frac{dR_{nq}}{dr}\right]_{r=r_n} - \left[k_1 rR_{1q}\frac{dR_{1p}}{dr} - k_1 rR_{1p}\frac{dR_{1q}}{dr}\right]_{r=r_0} + \sum_{i=1}^{n} k_i\int_{r_{i-1}}^{r_i} r\left(\lambda_{ip}^2-\lambda_{iq}^2\right)R_{ip}R_{iq}dr = 0 \tag{A-139}$$

At nth layer outer interface we have $R_n(r_n, t) = 0$

$$\left[k_n r R_{nq} \frac{dR_{np}}{dr} - k_n r R_{np} \frac{dR_{nq}}{dr}\right]_{r=r_n} = 0 \tag{A-140}$$

$$\left[k_1 r R_{1q} \frac{dR_{1p}}{dr} - k_1 r R_{1p} \frac{dR_{1q}}{dr}\right]_{r=r_0} = 0 \tag{A-141}$$

because $r_0 = 0$

Thus

$$\sum_{i=1}^{n} k_i \int_{r_{i-1}}^{r_i} r\left(\lambda_{ip}^2 - \lambda_{iq}^2\right) R_{ip} R_{iq} dr = 0 \tag{A-142}$$

$$\lambda_{ip} = \lambda_{1p} \sqrt{\frac{\alpha_1}{\alpha_i}} \tag{A-143}$$

Substitute Eq. A-143 into Eq. A-142.

$$\sum_{i=1}^{n} k_i \frac{\alpha_1}{\alpha_i} \int_{r_{i-1}}^{r_i} r\left(\lambda_{1p}^2 - \lambda_{1q}^2\right) R_{ip} R_{iq} dr = 0 \tag{A-144}$$

$$\alpha_1\left(\lambda_{1p}^2 - \lambda_{1q}^2\right) \sum_{i=1}^{n} \frac{k_i}{\alpha_i} \int_{r_{i-1}}^{r_i} r R_{ip} R_{iq} dr = 0 \tag{A-145}$$

or $p \neq q \rightarrow \left(\lambda_{1p}^2 - \lambda_{1q}^2\right) \neq 0$

Thus

$$\sum_{i=1}^{n} \frac{k_i}{\alpha_i} \int_{r_{i-1}}^{r_i} r R_{ip} R_{iq} dr = 0 \tag{A-146}$$

a_n can now be evaluated.

Apply initial condition to Eq. A-131

$$X_i = \sum_{n=1}^{\infty} a_n R_{in}(\lambda_{in} r) \tag{A-147}$$

Multiply both sides by $\frac{k_i}{\alpha_i} R_{iq}$ and integrate.

$$\frac{k_i}{\alpha_i} \int_{r_{i-1}}^{r_i} r X_i R_{iq} dr = \sum_{n=1}^{\infty} a_n \frac{k_i}{\alpha_i} \int_{r_{i-1}}^{r_i} r R_{in} R_{iq} dr \tag{A-148}$$

For n $\neq$ q we know that $\int_{r_{i-1}}^{r_i} r R_{in} R_{iq} dr = 0$

For n = q we have (also take summation of both sides for all layers i.e. from i =1 to k

$$\sum_{i=1}^{k} \frac{k_i}{\alpha_i} \int_{r_{i-1}}^{r_i} r X_i R_{in} dr = \sum_{i=1}^{k} a_n \frac{k_i}{\alpha_i} \int_{r_{i-1}}^{r_i} r R_{in}^2 dr \tag{A-149}$$

$$a_n = \frac{\sum_{i=1}^{k} \frac{k_i}{\alpha_i} \int_{r_{i-1}}^{r_i} r X_i R_{in} dr}{\sum_{i=1}^{k} \frac{k_i}{\alpha_i} \int_{r_{i-1}}^{r_i} r R_{in}^2 dr} \tag{A-150}$$

Thus Eq. A-96 is:

$$T_i = T_{ei} + \sum_{n=1}^{\infty} a_n \, e^{-\alpha_i \lambda_{in}^2 t} R_{in}(\lambda_{in} r) \tag{A-151}$$

Where a_n is given by Eq. A-150 and R_{in} is given by Eq. A-130.